Waste and Biomass Valorization
https://doi.org/10.1007/s12649-025-02894-0

ORIGINAL PAPER

Characterization of Magnesium-Iron Modified Biochar to Alleviate Ammonia Inhibition and Enhance Anaerobic Digestion of Chicken Manure

Tao Li[1,2,3,4] · Jinping Li[1,3,4] · Tingting Li[5] · Xiuwen Cheng[6]

Received: 1 August 2024 / Accepted: 5 January 2025

Abstract

Methane production from anaerobic digestion of chicken manure requires addressing the challenges posed by high nitrogen-containing substrates. One potential solution is the use of modified biochar to adsorb inhibitors and enhance the anaerobic digestion process. This study focused on preparing magnesium-modified biochar (Mg-BC), iron-modified biochar (Fe-BC), and magnesium-iron modified biochar (Mg/Fe-BC) through specific methods, and comparing their performance in simulated solutions for ammonia nitrogen adsorption. The results indicated that Mg/Fe-BC exhibited superior specific surface area, crystallinity, and functional groups compared to Mg-BC and Fe-BC. Its maximum adsorption capacity (87.83 mg/g) surpassed that of Mg-BC (26.77 mg/g) and Fe-BC (14.57 mg/g). Furthermore, the addition of 2%, 3%, and 5% Mg/Fe-BC to the biogas slurry resulted in NH_4^+-N removal efficiency of 16.38%, 32.85%, and 38.57%, respectively. In the anaerobic digestion test using chicken manure, adding 2%, 3%, and 5% Mg/Fe-BC effectively mitigated ammonia inhibition, leading to a substantial increase in cumulative methane production by 116%, 196%, and 229%, respectively. The addition also decreased the oxidation reduction potential, promoted the decomposition of volatile fatty acids and COD, and kept ammonia nitrogen within a final concentration range of 2.67–3.63 g/L, which helped maintain the stable operation of the system. Mg/Fe-BC facilitated the enrichment of acetogenic bacteria and enhanced the abundance of predominant archaea, including *Methanosarcina* and *Methanosaeta*. These findings provided valuable insights into the ammonia nitrogen adsorption characteristics of Mg/Fe-BC and its effectiveness in enhancing methane production from chicken manure anaerobic digestion.

Highlights

- A novel biochar modification technique was developed for enhancing the anaerobic digestion of chicken manure.
- Mg/Fe-BC exhibited relatively high efficiency in removing ammonia nitrogen from simulated solution and slurry.
- The addition of 2-5% Mg/Fe-BC can alleviate the inhibition of ammonia nitrogen and promote methane production by 116-229%
- Mg /Fe-BC increase the relative abundance of *Methanosarcina* and *Methanosaeta* in anaerobic digestion of chicken manure.

✉ Jinping Li
lijinping77@163.com

[1] School of Energy and Power Engineering, Lanzhou University of Technology, Lanzhou 730050, China

[2] Jiuquan Vocational Technical College, Jiuquan 735000, China

[3] Collaborative Innovation Center for Supporting Technology of Northwest Low-Carbon Towns, Lanzhou 730050, China

[4] Gansu Key Laboratory of Complementary Energy System of Biomass and Solar Energy, Lanzhou 730050, China

[5] Food Test Center of Jiuquan, Jiuquan 735000, China

[6] College of Earth and Environmental Sciences, Lanzhou University, Lanzhou 730050, China

Published online: 28 January 2025

Graphical Abstract

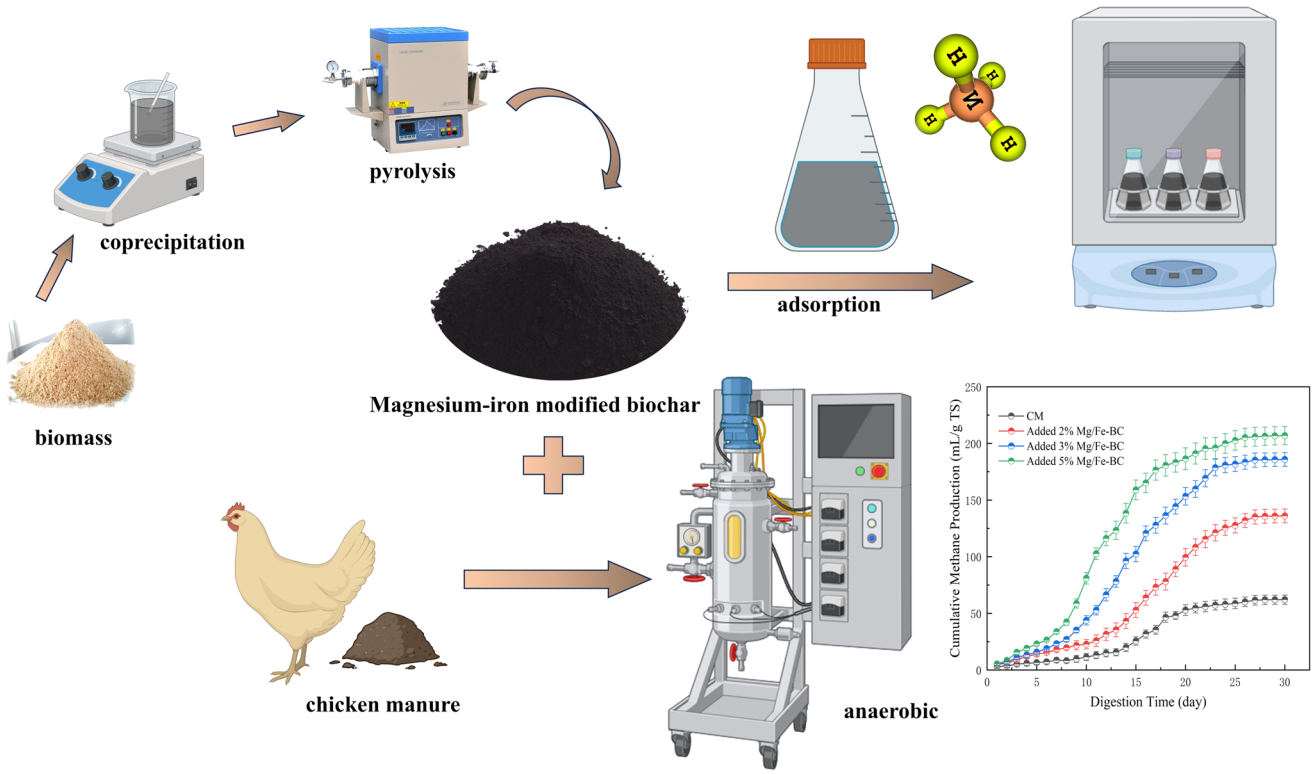

Keywords Modified biochar · Adsorption capacity · Anaerobic digestion · Cumulative methane production · Ammonia inhibition

Introduction

The exponential growth of livestock and poultry farming has presented significant challenges in managing their manure. With its large volume, high organic content, and potential pathogenic bacteria, untreated disposal poses a grave threat to ecosystem environment and economic development [1]. To solve this problem, the adoption of proper treatment methods and recycling strategies is crucial to mitigate environmental harm and foster sustainable industry growth. Anaerobic digestion (AD) has emerged as a promising renewable energy technology, reducing reliance on fossil fuels by converting organic waste into clean bioenergy [2]. The resultant digestate from manure fermentation is nutrient-rich, containing valuable elements like nitrogen and phosphorus that can be beneficial in agricultural applications [3]. AD not only aids in waste reduction and minimizes greenhouse gas emissions but also produces organic fertilizers, diminishes malodorous gases, and generates renewable methane [4, 5]. Consequently, AD is increasingly acknowledged as a favorable waste management solution aligned with the principles of a green, low-carbon circular economy [5].

The stability of AD relies on the complex interactions among various bacteria and archaea, as well as the balance between methanogenic stages. Anaerobic microorganisms are vulnerable to adverse conditions and toxic substances [6, 7]. However, high levels of ammonia nitrogen (AN), a crucial metabolic byproduct from the AD of chicken manure (CM), can inhibit methane production. AN inhibition is a significant technical challenge that restricts AD biogas production, as it severely hampers bacterial activity and impedes the degradation of volatile fatty acids (VFA), further hindering methane production [8]. Overcoming the obstacles of high ammonium nitrogen levels, toxic substrate inhibition, and VFA accumulation is essential for maintaining the stability and continuity of AD [9, 10]. Various methods such as microbial-mediated nitrification and denitrification, zeolite ion exchange [11], chemical precipitation of struvite [12], gas-lift techniques [13], and the use of biochar from different sources have been implemented to reduce total ammonia nitrogen (TAN) in AD [14, 15]. Additionally, the incorporation of metal-based materials into anaerobic reactors shows

promise in enhancing the operational stability of the AD system [16, 17]. It is worth considering that in the ammonia recovery strategy, we need to overcome the shortcomings of physical and chemical methods in terms of operating conditions and costs. Farghali et al. reported that the integrated physical and chemical mixing process could improve the ammonia removal efficiency of wastewater, especially the collaboration between nitrification and ammonia anaerobic digestion in membrane bioreactors, which had shown an efficient and promising approach [18].

Biochar (BC), a novel type of adsorbent, possesses exceptional properties including a stable structure, large specific surface area, and abundant functional groups [19]. The production of recycled products from agricultural waste and various waste streams has become a popular trend. For example, Akor et al. [20] studied the potential of AD residue solid digestate as a potential solid biofuel, and Osman et al. [21] quickly synthesized highly active magnetic adsorbent composite materials using plastic bottle waste and fruit residue biomass waste. Only by improving the application value of biomass derivatives can greater economic benefits be achieved. The adsorption capacity of BC for AN is influenced by various physicochemical properties such as surface area, cation exchange capacity, ash content, and chemical bonding [22, 23]. BC plays a key role in mitigating TAN buildup and accumulation through its surface functional groups or pore structure, which are utilized for direct adsorption of NH_4^+ as well as microbial colonization. This dual action of adsorption reduces the bioavailability of NH_4^+ to methanogens, while also providing protection to methanogens from ammonia nitrogen inhibition in the environment. Generally, a positive correlation has been observed between the addition of BC and the reduction of TAN. Yu et al. [24] demonstrated that a 1% by volume dose of biochar led to a significant 19.5% reduction in TAN, whereas a study by Pan et al. [25] found that a 5% by volume dose of biochar could reduce TAN by up to 25%. The introduction of divalent and trivalent metal co-modification can lead to the formation of layered double oxides and facilitate the creation of more adsorption sites in biochar. It also possesses specific advantages such as anion exchange, cation compatibility, and hydroxyl enrichment.

The modified biochar is capable of removing ammonia nitrogen complexed with oxygen-containing functional groups (such as carboxyl, phenol, etc.) through pore filling and surface adsorption [26]. Additionally, NH_4^+ can interact with the surface of negatively charged ions via electrostatic attraction and physical adsorption of biochar adsorbent materials [27]. Magnesium-iron biochar composites have significant adsorption capacity for pollutants in wastewater. It has been reported that the molar ratio of Mg^{2+}: Fe^{3+} in the synthesis of Mg/Fe-BC is typically 2:1, which can enhance the safety of biochar and reduce the risk of metal leaching [28]. Bian et al. prepared Mg/Fe-BC for the removal of ammonia nitrogen and phosphorus in biogas slurry, with efficiencies of up to 30.0% and 81.8%, respectively [29]. He et al. used phosphorus-containing biochar adsorbent in biogas production from swine manure, reducing the ammonia nitrogen content to 200 mg/L [30]. Moreover, the promotion of AD by magnesium-iron modified biochar is not limited to ammonia nitrogen adsorption. Enhancing direct interspecies electron transfer (DIET) is also an important reason for improving the efficiency of AD systems under ammonia stress. Combining DIET with AD can improve the efficiency of converting large molecules into organic acids and CH_4, thereby increasing biogas production [31]. Metal-modified biochar can serve as a conductive material to promote DIET, thereby improving methanogenesis in NH_3-stressed AD systems. Through its high surface area, reactivity, and specificity, modified biochar increases the number of active sites for species such as *Bacillus* ground and *methanobacterium*, facilitating the direct contact necessary for efficient electron transfer between species [31].

Despite the evident advantages of employing magnesium-modified biochar for pollutant removal in water environments, the economics and environmental sustainability of large-scale production and preparation procedures still encounter significant challenges. The activation and synthesis of bimetal-loaded biochar-based materials require overcoming the high costs of raw materials and the environmental pollution caused by chemical residues [32]. Nevertheless, the regeneration performance and reuse of magnesium iron modified biochar still hold potential value. For instance, Hu et al. reported that magnetic biochar still maintains a strong adsorption capacity after four cycles of recycling [33]. Ji et al., through intermittent experiments and fixed-bed continuous flow experiments, disclosed that the penetration time of Fe/Mg-WHBC to imidacloprid was merely reduced by 27.6% after five adsorption-regeneration cycles [34]. Regarding environmental sustainability, life cycle analysis and carbon sequestration potential assessment were conducted on the pyrolysis production of magnesia-based biochar to develop carbon removal projects with environmental benefits. For example, Fawzy et al. evaluated the economy of atmospheric carbon removal through large-scale pyrolysis OTPR in Spain, providing references for addressing the climate crisis [35].

In this study, Magnesium/iron modified biochar was synthesized through chemical precipitation and post-pyrolysis, and its physical and chemical properties were subsequently examined. The adsorption capacity of ammonia nitrogen in

both simulated solution and real biogas slurry was evaluated and compared. Additionally, varying amounts of modified biochar were introduced into the chicken manure AD system to investigate the efficacy of modified biochar in enhancing the gas production performance of high ammonia nitrogen anaerobic digestion. Moreover, the microbial community structure in the AD system was also analyzed. The study aims to clarify the key roles and mechanisms of functional biochar in promoting methane production during anaerobic digestion and provide new insights.

Materials and Methods

Preparation of Magnesium-iron Modified Biochar

Corn cobs was harvested from a farm in Jiuquan, China, air-dried to remove impurities, crushed through a 100-mesh sieve, and stored in a sealed container. A quantity of 50 g of corncob biomass was then placed into a solution containing 0.2 mol/L $FeCl_3$•$6H_2O$ and 0.4 mol/L $MgCl_2$•$6H_2O$, and subjected to ultrasonication at room temperature for 30 min. Subsequently, the pH was adjusted to 10 using a 2.5 mol/L NaOH solution, followed by an aging process at 60 °C for 12 h. The solid mixture obtained after filtration was washed with deionized water, then dried in an oven at 60 °C for 24 h. The biochar was finally produced through pyrolysis in a vacuum tubular furnace (HFRG 8.120), with a heating rate of 10 °C/min, nitrogen flow rate of 200 mL/min, and pyrolysis sustained at 500 °C for 2 h [29]. The magnesium-iron modified biochar obtained was defined as Mg/Fe-BC, magnesium-modified biochar (Mg-BC) without the addition of $FeCl_3$•$6H_2O$, and iron-modified biochar (Fe-BC) without the addition of $MgCl_2$•$6H_2O$, all other preparation steps remained the same.

Characterization of Modified Biochar

The surface morphology of the modified biochar was observed using a scanning electron microscope (SEM) (Gemini SEM 500, Germany), while surface elements were detected using an energy spectrometer (EDS) (Oxford Ultim Max 100, UK). Elemental content was analyzed using an organic elemental analyzer (Elementar Vario Micro Cube, Germany), and the specific surface area and pore size characteristics were examined through Bruner Emmett Taylor (BET) analysis (Micromeritics ASAP2420, USA). The crystal structure of the modified biochar on the surface was determined using an X-ray diffractometer (XRD) (D8 Discover, Bruker, Germany). Functional groups was characterized using Fourier transform infrared spectroscopy (FTIR) (Nicolet iS5, USA).

Adsorption Experiment

To examine the impact of varying dosages of modified biochar on NH_4^+-N removal efficiency, 0.5–5 g/L of modified biochar was added to 100 mL of ammonium chloride solution with an initial concentration of 120 mg/L. The mixture was then allowed to react for 24 h at a speed of 150 rpm in a thermostatic shaking chamber maintained at 25 °C. To observe the trend of NH_4^+ adsorption changing over time, add 1 g/L of modified biochar to a 100mL solution containing 120 mg/L of ammonium chloride. Take samples at 5, 10, 15, 30, 60, 120, 240, 480, 720, and 1440 min to measure the concentration of ammonia nitrogen. Isothermal adsorption experiment was conducted under consistent conditions with initial NH_4^+ concentrations ranging from 40 mg/L to 1000 mg/L. The kinetic model and isothermal adsorption model are elaborated in Text S1&S2. Additionally, 100 mL of biogas was utilized to adjust the ammonia nitrogen concentration to 1500 mg/L. Subsequently, 2.0%, 3.0%, and 5.0% of Mg/Fe-BC were introduced to assess the removal efficiency of Mg/Fe-BC on ammonia nitrogen in the biogas. The concentration of ammonia nitrogen was measured at 420 nm using the Nano reagent spectrophotometric method outlined by the State Environmental Protection Administration of China (HJ-2009). The experiment was conducted in triplicate. The adsorption capacity at equilibrium (Q_e, mg/g) and removal efficiency (R, %) were calculated by the following Eq. [2]:

$$Q_e = \frac{(C_0 - C_e)\,V}{M} \tag{1}$$

$$R = \frac{(C_0 - C_e)}{C_0} \times 100\% \tag{2}$$

where C_0 (mg/L) and C_e (mg/L) are NH_4^+-N concentrations at initial time and equilibrium, V (L) is the solution volume, and M (g) is the adsorbent weight.

Anaerobic Digestion Experiment

Experiment Device

The anaerobic digestion device used in this study was a fully automatic quadruple 10 L stainless steel anaerobic reactor, manufactured by BeiJing ManCang Technology Co., Ltd (Fig. S1). The anaerobic digestion was conducted at a constant temperature of 37 ± 1°C. Before starting, the airtightness of the device was verified, and the effective working volume of each fermentation tank was 7.5 L, with a stirring speed set at 40 rpm/min. The first anaerobic reactor used only chicken manure as a substrate. The second, third,

and fourth tanks added 2%, 3%, and 5% magnesium iron modified biochar (refer to the percentage of added amount to the total digestate weight), respectively, labeled as CM, 2%Mg/Fe-BC, 3%Mg/Fe-BC, and 5%Mg/Fe-BC. Real-time parameters monitored during the anaerobic digestion included pH value, oxidation-reduction potential (ORP), cumulative biogas production, and cumulative methane production in the fermentation broth.

Substrate and Inoculum

Fresh chicken manure was collected from a laying hen farm in Jiuquan City, China, and stored in a 4 °C refrigerator after removing debris. The inoculum used was obtained from the Key Laboratory of Biomass and Solar Complementary Energy Supply System in Gansu Province at Lanzhou University of Science and Technology. The inoculum was domesticated and cultured in an anaerobic reactor before use. The initial substrate loading of the anaerobic digestion was maintained at 50 g TS/L, with the chicken manure and inoculum mixed in a ratio of 2:1 (based on TS). The specific properties of the chicken manure feedstock, inoculant, and mixed substrate are detailed in Table 1.

Sample Analysis Methods

Biogas and methane production, pH, and ORP were monitored daily, while COD, NH_4^+-N, and VFA content were analyzed every 3 days. Liquid samples were centrifuged at 10,000 rpm for 10 min, with the supernatant used for COD and NH_4^+-N concentration analysis. Ammonia nitrogen concentration was determined using the standard Nano reagent spectrophotometric method (HJ-2009), and COD concentration was determined using the dichromate method (HJ 828–2017) as specified by the State Environmental Protection Administration of China. Cumulative methane content was measured with a methane analyzer (Biogas 5000, Germany). Liquid samples were further processed by centrifuging at 10,000 rpm for 10 min, followed by filtration through 0.45 μm and 0.22 μm membrane filters for VFA analysis. VFA analysis was conducted using gas chromatography (Shimadzu GC-2014) with a FID detector and a Wonda Cap FFAP (30 m × 0.25 mm × 0.25 μm) capillary column [36].

Methane Production Simulation

Modified Gompertz Eq. (3) was used to describe methane production and stated the methane potential, maximum methane production, and lag-phase time [37].

:

$$M = P_m exp\left\{-exp\left[\frac{R_m \times e}{P_m}(\lambda - t) + 1\right]\right\} \quad (3)$$

where M is the cumulative methane production (mL), P_m is methane production potential (mL), R_m is the maximum methane production rate (mL/d), λ is the lag-phase time (d), t is the anaerobic digestion time (d), and e is the natural constant.

Microbial Community Analysis

At the end of the AD experiment, digestates were collected for the analysis of the bacterial and archaea communities. DNA samples were acquired using the Mag-Bind soil DNA kit (Omega Bio-Tek, USA). The extracted DNA samples underwent 16 S rRNA high-throughput sequencing and PCR amplification with bacterial primers 338 F and 806R and archaea primers 524 F10 extF and Arch958 RmodR [38]. PCR products were combined with an equal volume of 1×loading buffer and analyzed through electrophoresis on 2% agarose gel. After purification with a paramagnetic bead (Agencourt AMPure XP, Beckman Coulter, USA), the concentration of DNA was determined using a fluorometer device (Qubit 2.0, FEI, USA). Paired end sequencing of PCR products was carried out using the Illumina Miseq platform at Sangon Biotech in Shanghai, China.

Results and Discussion

Physicochemical Properties of Modified Biochar

The elemental contents and atomic ratios of BC, Mg-BC, Fe-BC, and Mg/Fe-BC were presented in Table 2. The decrease in C, H, and O content in magnesium and iron modified biochar was attributed to the escape of H and

Table 1 Physical and chemical properties of chicken manure, inoculum and mixed substrate

Parameters	Unit	Chicken manure	Inoculum	Anaerobic Digestion Mixture
Chemical Oxygen Demand (COD)	g/L	47.6	6.64	30.53
Total Solids (TS)	%	39.02	4.17	13.45
Volatile Solid (VS)	%	23.41	2.88	9.14
pH	-	7.55	7.86	7.32
Electrical Conductance (EC)	ms/cm	11.02	7.68	15.26
Oxidation Reduction Potential (ORP)	mv	-324.13	-375.76	-267.68
Ammonia Nitrogen (NH_4^+-N)	mg/L	5634.24	946.93	1279.45
Soluble Phosphorus (PO_4^{3-}-P)	mg/L	426.51	224.72	278.63

Table 2 Surface morphology parameters and elemental composition of biochar

Sample	BET (m^2/g)	Pore volume (cm^3/g)	Pore size (nm)	Elemental content						
				C(%)	H(%)	O(%)	*N*(%)	O/C(%)	H/C(%)	(O+*N*)/C(%)
BC	3.4344	0.0134	13.9154	71.19	3.43	22.62	0.59	0.32	0.05	0.33
Mg-BC	32.9362	0.1013	11.2505	53.43	3.85	20.66	0.38	0.39	0.07	0.39
Fe-BC	27.0909	0.0795	11.7361	51.62	2.26	20.86	0.26	0.40	0.04	0.41
Mg/Fe-BC	71.6935	0.1574	9.3505	48.4	1.85	17.87	0.25	0.37	0.04	0.37

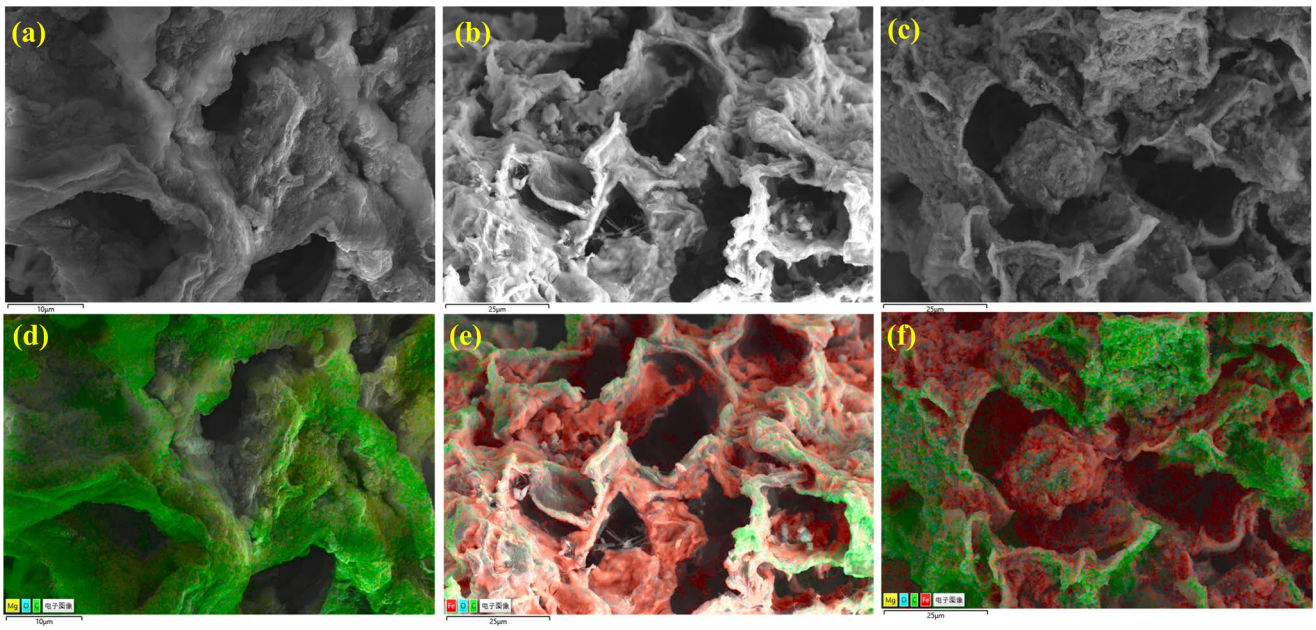

Fig. 1 SEM-EDS images of Mg-BC (**a**, **d**), Fe-BC (**b**, **e**), Mg/Fe-BC (**c**, **f**)

O elements as gas-phase fractions (H_2, CO, and CO_2), resulting in a slight reduction in H and O content [39]. However, the O/C and (O + N)/C values were found to be higher in Mg-BC, Fe-BC, and Mg/Fe-BC when compared to BC, without exceeding 0.6 [40]. This suggested higher hydrophilicity and polarity [41]. The data in Table 2 highlighted a significant increase in the specific surface area of the modified biochar, particularly in Fe/Mg-BC where the specific surface area reached 71.6935 m^2/g, approximately 21 times higher than that of the BC. Additionally, the pore volume of Fe/Mg-BC increased by about 15 times to 0.1574 cm^3/g. This expansion in surface area and pore volume provided more adsorption sites for ammonia nitrogen and phosphate in the slurry. The porosity and specific surface area of modified biochar have significant influences on the adsorption of ammonia nitrogen. Porosity and specific variable area are positively correlated with physical adsorption. Porosity affects the physical adsorption of ammonia nitrogen through intra-particle diffusion, and the specific surface area mainly influences the surface adsorption capacity [42].

However, it was observed that the average pore size of the Mg/Fe-BC decreased due to pore blockage caused by metal deposits [43]. SEM images (Fig. 1) revealed a rough surface texture on the modified biochar with numerous folds and irregular pore structures, which were crucial for pollutant adsorption. SEM-EDS analysis (Fig. 1d-f) demonstrated a uniform distribution of metal elements on the modified biochar surface, with noticeable granularity around voids. The pyrolysis process enhanced the bonding of magnesium and iron with the raw biochar, resulting in a significant presence of metal oxide deposits. These findings confirmed the successful loading of magnesium and iron oxides onto the raw biochar. The metal oxides deposited on the surface can increase the specific surface area, and the formed Mg-O/Fe-O functional groups provide a new active site, thus increasing the adsorption capacity [44], which will be discussed in detail in the following chapters.

XRD and FTIR Analysis

The crystal structures of Mg-BC, Fe-BC, and Mg/Fe-BC were analyzed using XRD. In Fig. 2a, two sharp broad peaks at 2θ = 42.91° and 62.29° were observed, corresponding to the characteristic peaks of MgO, indicating

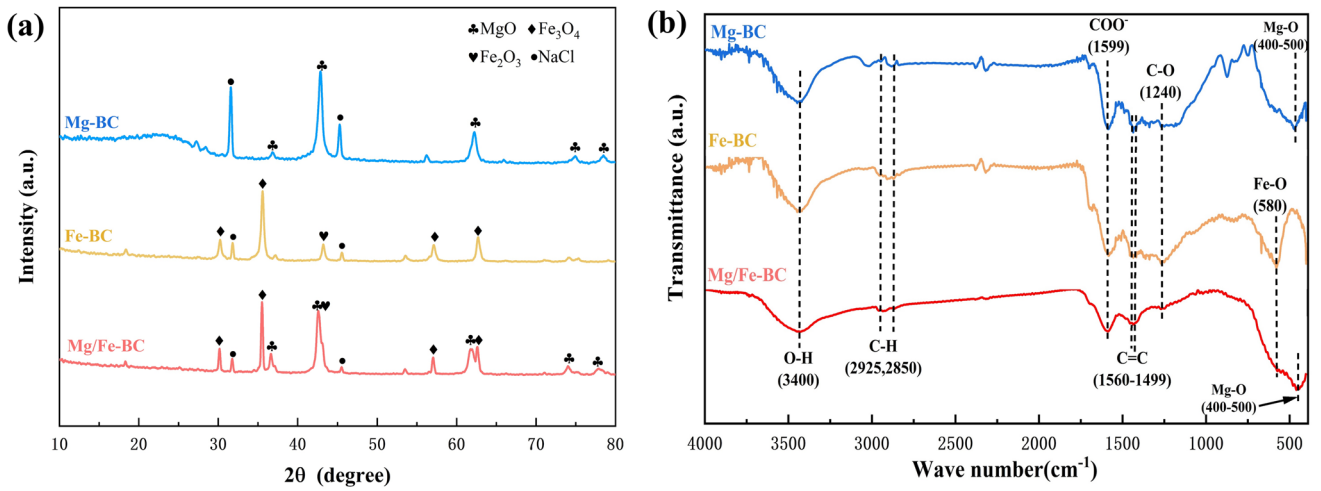

Fig. 2 XRD (**a**) and FTIR (**b**) spectra of different modifoied biochar

successful loading of magnesium oxide onto the biochar surface [45]. Peaks at 2θ = 30.05, 35.39, 43.01, 56.87, and 62.45 were identified as Fe_3O_4 or Fe_2O_3, suggesting effective binding of iron to the biochar [46]. Similarly, Mg/Fe-BC exhibited diffraction peaks of magnesium oxide and magnetite at the same 2θ value. A diffraction peak of NaCl was also observed at 31.66 for all three modified biochars, likely due to the presence of alkali metal elements in the corn cob material. FTIR analysis revealed abundant functional groups on the surfaces of Mg-BC, Fe-BC, and Mg/Fe-BC (Fig. 2b). The spectral bands at 3400 cm^{-1}, 2925 cm^{-1}, and 2850 cm^{-1} were attributed to -OH stretching and $-CH_2$ bending vibrations [47]. The characteristic peak at 1599 cm^{-1} corresponded to COO-, where the negatively charged acidic functional group interacted with cationic ammonium species and exchanges H^+ on the biochar surface [48]. The stretching vibration at 1560–1499 cm^{-1} was related to C = C, while the absorption peak at 1240 cm^{-1} was mainly due to C-O bonds [45]. Additionally, the bands at 580 cm^{-1} and 400–500 cm^{-1} were associated with Fe-O and MgO vibrations, respectively, providing further evidence of successful loading of iron and magnesium [49, 50]. Oxygen-containing functional groups, such as hydroxyl and carboxyl groups, primarily influence chemisorption and significantly contribute to ammonia nitrogen adsorption [51, 52]. Furthermore, the ion exchange capacity is positively correlated with the oxygen-containing functional groups. The alkali metals (Na^+, K^+, Mg^{2+}) on the surface of the modified biochar exchange metal ions with NH_4^+, facilitating the adsorption of ammonia nitrogen in the AD system [51, 53]. Hence, the increase of functional groups on the surface of biochar after metal modification enhances its polarity, which is beneficial for the chemical adsorption of ammonia nitrogen.

Adsorption Performance of Modified Biochar on Ammonia Nitrogen

The impact of varying biochar dosages on the efficiency of removing ammonia nitrogen was illustrated in Fig. 3a. Under room temperature conditions (25 ± 3 °C), the removal efficiency of NH_4^+-N increased with higher dosages of all three types of modified biochar. In particular, as the dosage of modified biochar rose from 0.5 g/L to 3.0 g/L, there was a noticeable enhancement in the removal efficiency of NH_4^+-N. The removal efficiency percentages for Mg-BC, Fe-BC, and Mg/Fe-BC were 36.51%, 18.31%, and 60.57%, respectively. Further increasing the dosage to 5.0 g/L resulted in a slower increase in removal efficiency, ultimately reaching 38.39%, 19.45%, and 63.00%, respectively. This trend was attributed to the ample adsorption sites provided by the modified biochar, leading to saturation of adsorption sites and subsequent stabilization of ammonia nitrogen removal efficiency [54]. Obviously, Mg/Fe-BC showed the highest efficiency in removing ammonia nitrogen, suggesting its potential superiority in adsorption and immobilization within AD systems.

The NH_4^+-N adsorption process was investigated through adsorption kinetic model, with pseudo-first-order model and pseudo-secondary-order model used to analyze the experimental data. Figure 3b illustrated that NH_4^+-N adsorption initially occurred rapidly, then slowed down before reaching equilibrium. The Mg-BC and Fe-BC reached equilibrium in approximately 4 h, while Mg/Fe-BC approached equilibrium gradually over 8 h, exhibiting a significantly higher adsorption capacity than the former. The kinetic fitting parameters presented in Table 3 indicated that the adsorption capacity (Q_e) of Mg-BC, Fe-BC, and Mg/Fe-BC were 19.48 mg/g, 8.81 mg/g, and 57.73 mg/g, respectively. This revealed that Mg/Fe-BC had a superior adsorption capacity.

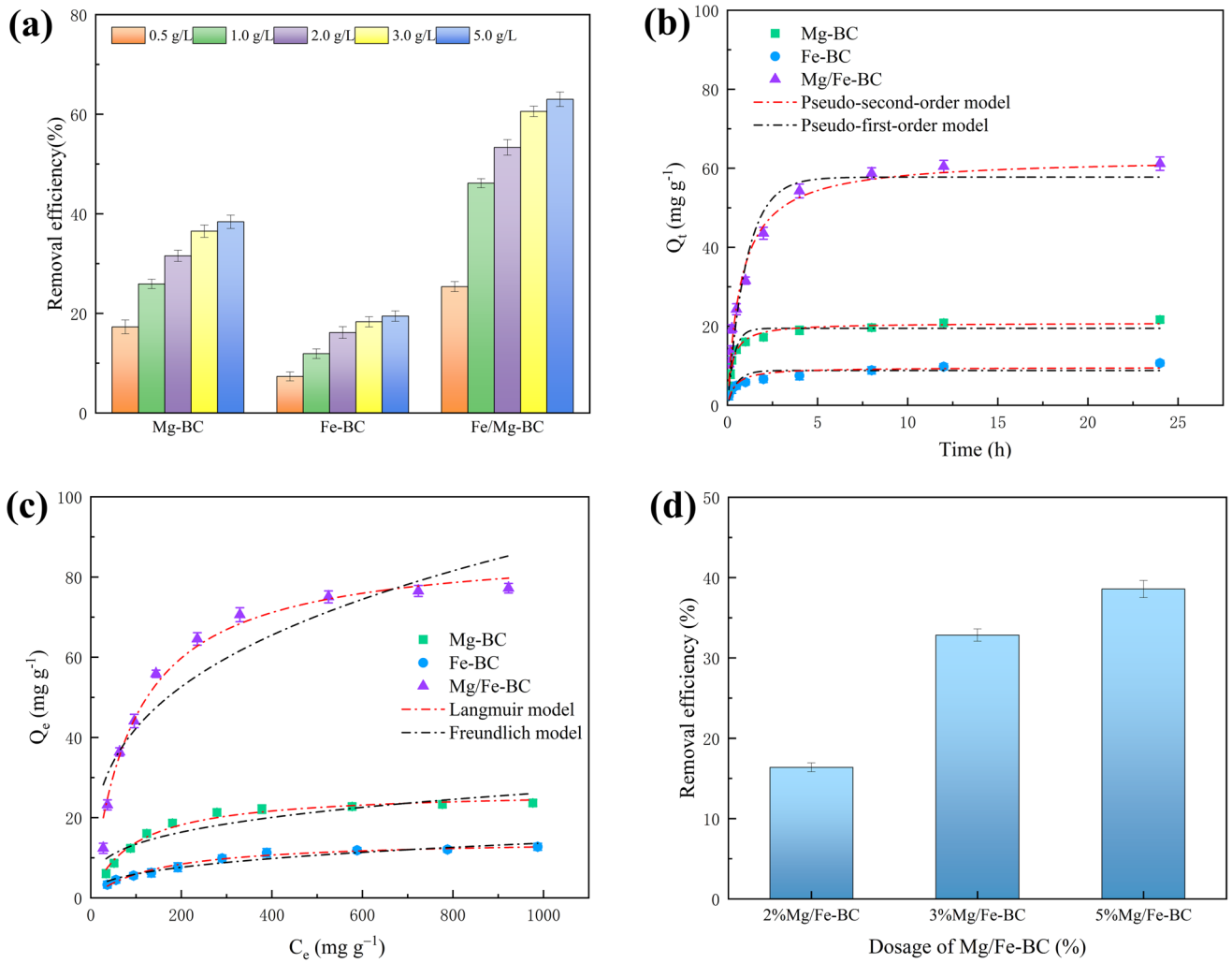

Fig. 3 The effect of modified biochar dosage on ammonia nitrogen removal efficiency (**a**); adsorption kinetics of Mg-BC, Fe-BC, and Mg/Fe-BC (**b**); adsorption isotherms of Mg-BC, Fe-BC, and Mg/Fe-BC (**c**); the removal efficiency of ammonia nitrogen in biogas slurry with different Mg/Fe-BC addition levels (**d**)

Table 3 Adsorption kinetic parameters of Mg-BC, Fe-BC, and Mg/Fe-BC

Modified biochar	Pseudo-first-order model			Pseudo-second-order model		
	k_1	Q_e (mg/g)	R^2	k_2	Q_e (mg/g)	R^2
Mg-BC	2.7194	19.4826	0.8733	0.1828	20.8540	0.9706
Fe-BC	1.9302	8.8090	0.7415	0.2600	9.5790	0.8925
Mg/Fe-BC	0.9459	57.7269	0.9215	0.0209	62.6595	0.9669

Moreover, the R^2 values of the pseudo-secondary-order model for the three modified biochars were higher than those of the pseudo-first-order model. This suggested that NH_4^+-N adsorption conformed to the pseudo-secondary-order kinetic model, implying that NH_4^+-N adsorption might be primarily a chemical process driven by ion exchange [55].

The adsorption capacity of the three modified biochars with varying initial concentrations of NH_4^+-N were depicted in Fig. 3c. The data was analyzed using Langmuir and Freundlich models, with results presented in Table 4 indicating that the Langmuir model ($R^2 = 0.98–0.99$) was a better fit for the NH_4^+-N adsorption process. This suggested a monomolecular layer adsorption mechanism rather than a multilayer non-homogeneous phase adsorption. The maximum adsorption capacities (Q_m) of Mg-BC, Fe-BC, and Mg/Fe-BC were determined to be 26.78 mg/g, 14.57 mg/g, and 87.83 mg/g, respectively. Notably, the maximum adsorption capacity of Mg/Fe-BC was significantly higher than that of Mg-BC and Fe-BC, consistent with findings from previous studies [2, 56, 57]. These results affirmed the superior adsorption effectiveness of Mg/Fe-BC towards NH_4^+-N.

Table 4 Adsorption isothermal model parameters of Mg-BC, Fe-BC, and Mg/Fe-BC

Modified biochar	Langmuir model				Freundlich model	
	Q_m (mg/g)	K_L (L/mg)	R^2	K_F (mg/g)	1/*n*	R^2
Mg-BC	26.7677	0.0106	0.9800	3.4876	0.2920	0.8514
Fe-BC	14.5692	0.0069	0.9865	1.1220	0.3619	0.9504
Mg/Fe-BC	87.8300	0.0107	0.9789	9.8816	0.3157	0.8489

The complexity of real AD processes surpassed that of simulated NH_4^+-N solutions. This study evaluated the NH_4^+-N adsorption capability by adjusting the NH_4^+-N concentration in chicken manure slurry to 1500 mg/L and adding varying amounts of Mg/Fe-BC [38]. The results, illustrated in Fig. 3d, indicated that NH_4^+-N removal rates were 16.38% ± 0.54%, 32.85% ± 0.76%, and 38.57% ± 1.06% for Mg/Fe-BC dosages of 2%, 3%, and 5% respectively. Obviously, a 5% Mg/Fe-BC dosage effectively reduced NH_4^+-N concentration in the slurry, suggesting that Mg/Fe-BC could regulate NH_4^+-N levels through adsorption and desorption processes, thereby maintaining a lower ammonia nitrogen load. Previous research found that the pH of Mg/Fe-BC was approximately 8.23, which favored rapid adsorption of NH_4^+ [58]. Consequently, the adsorption of NH_4^+-N by Mg/Fe-BC could play a role in stabilizing AD processes or mitigating ammonia inhibition.

The kinetic and isothermal models of magnesium and iron modified biochar confirm that the adsorption reaction encompasses both chemisorption and physical adsorption. The porous structure (SEM-EDS) and the large rough surface (BET) of Mg/Fe-BC generate numerous active sites for ammonia nitrogen binding. XRD and FTIR analysis reveal that more oxygen-containing functional groups (such as -OH, C-O, C = O, Mg-O and Fe-O groups) are involved in the adsorption of NH_4^+, and the mechanisms mainly include electrostatic attraction, surface precipitation and ion exchange [59]. Biogas slurry is typically alkaline. When $pH > pH_{ZPC}$, NH_4^+ in the AD system can be electrostatically attracted by the modified biochar with negative surface charge, and the adsorption amount of NH_4^+ increases along with the rise of the pH value of the solution [60, 61]. Additionally, due to the presence of phosphate in the actual biogas slurry, Mg^{2+} doped in the biochar can be better facilitated to combine with ammonia nitrogen to form guanolite, and the surface precipitation mechanism can promote the removal of ammonia nitrogen in the AD system [62]. A large number of studies have discovered that ion exchange is the principal mechanism for the adsorption of ammonium by Mg/Fe-BC. Alkali metals as exchangeable cations influence the cation exchange capacity, Mg/Fe-BC participates in the adsorption of ammonium through Mg^{2+} exchange, and the functional groups on its surface have a significant impact on the removal of ammonia nitrogen [63].

Biogas and Methane Production Performance

Figure 4 illustrated the impact of varying dosages of Mg/Fe-BC on biogas production, methane production, and methane content during CM anaerobic digestion. The results clearly showed that both biogas and methane production increased with the addition of Mg/Fe-BC (Fig. 4a, b). Biogas and methane production in the CM-only anaerobic reactor remained almost unchanged from 1 to 12 days. There was a slight recovery observed in the subsequent 15–20 days; however, biogas production and methane yield remained low during the final stage of anaerobic digestion. The cumulative biogas production and methane production were recorded at only 133.05 ± 7.98 mL/g TS and 62.08 ± 4.08 mL/g TS. These results indicated that the anaerobic digestion of CM-only faced significant inhibition due to the high-nitrogenous and easily acidifiable nature of the organic substrate [64].

After adding 2.0% Mg/Fe BC, a slight increase in biogas production was observed, with biogas and methane production of 216.39 ± 9.02 mL/g TS and 135.98 ± 6.08 mL/g TS, respectively. The initiation of the biogas production process was slow, but the trend of methanogenic development was clearly different from that seen with CM-only conditions. It was evident that the addition of Mg/Fe-BC could promote the stabilization of AD performance, as Mg/Fe-BC facilitated the transition of anaerobic digestion from an unstable state to normal biogas production. This beneficial effect was attributed to the enhancement of CM anaerobic digestion by various abiotic additives such as biochar, biomass ash, and minerals [14, 65]. When the Mg/Fe-BC addition was 3.0%, there was a significant increase in cumulative biogas and methane production. Biogas production began rapidly within the first 10 days, with cumulative biogas production and methane production reaching near maximum levels by day 26, ultimately reaching 292.56 ± 8.86 mL/g TS and 183.78 ± 6.18 mL/g TS, respectively. Biogas production and methane production saw an increase of approximately 115% and 187%, respectively. With a 5% Mg/Fe-BC addition, there was a slight enhancement in biogas production and cumulative methane production. Interestingly, starting from the 6th day, the cumulative biogas and methane production increased at a faster rate compared to the 3% addition amount. By the 24th day, the cumulative biogas and methane production were close to their maximum, ultimately

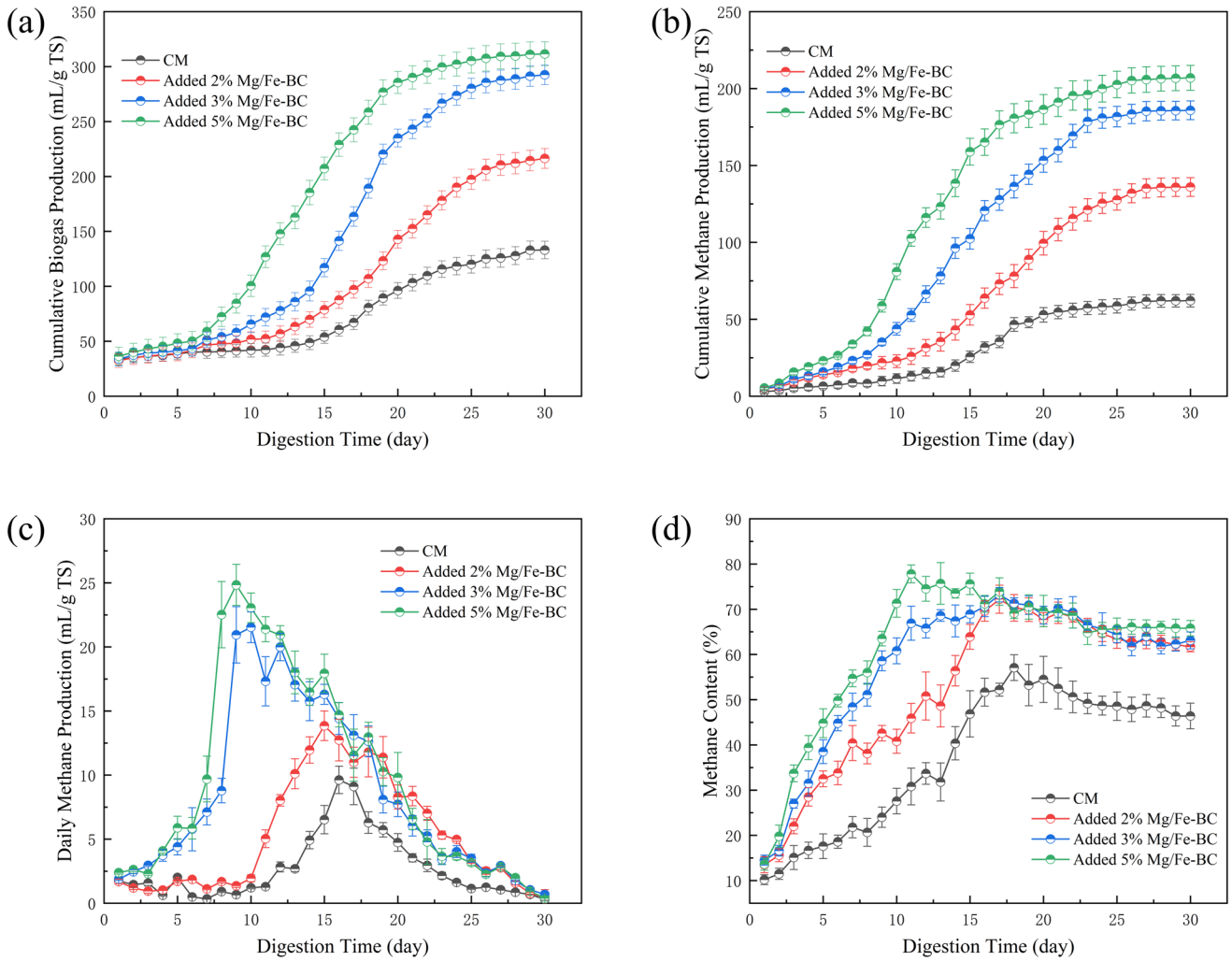

Fig. 4 The effect of Mg/Fe-BC addition on the anaerobic digestion gas production performance of chicken manure. (**a**) cumulative biogas production; (**b**) cumulative methane production; (**c**) daily methane production; (**d**) variations in methane content

reaching 311.48 ± 11.02 mL/g TS and 206.94 ± 8.10 mL/g TS, with increases of up to 133% and 228%, respectively. These results further confirmed that magnesia-iron modified biochar could enhance the degradation rate of organic substrates and methane production. The addition of modified biochar in the AD system could mitigate inhibitory phases, improve process stability, aid in adsorption of toxic compounds, enhance buffering capacity, and support the immobilization of anaerobic bacteria [66, 67].

Daily methane production was observed in all four groups of anaerobic digesters throughout the 30 days cycle (Fig. 4c). In the anaerobic reactor with only CM, daily methane production remained stagnant for the first 11 days, then peaked on the 16th day at 9.55 ± 1.07 mL/g TS before gradually decreasing to zero. The addition of 2% Mg/Fe-BC showed a similar methanogenesis trend to the CM group, but started 1–2 days earlier, reaching a peak on the 15th day at 13.44 ± 1.15 mL/g TS. Daily methane production continued until the 20th day before declining. This suggested potential inhibition in the anaerobic digestion of CM, likely due to high ammonia nitrogen concentration [68]. The groups with 2% and 3% Mg/Fe-BC had significantly higher daily methane production, peaking on days 9–10 at 21.68 ± 1.20 mL/g TS and 25.64 ± 1.61 mL/g TS, respectively, and remaining high until the 18th day. This indicated that Mg/Fe-BC addition could enhance methanogenesis, consistent with previous research [14, 69].

Figure 4d illustrated the changes in methane content over the 30d anaerobic digestion period. Initially, methane content increased to a peak, then gradually declined before stabilizing. This trend was consistent with daily methane production. Methane content in CM was below 50% for the first 15 days, peaking at 57.08 ± 2.84% on the 18th day. The addition of 2% Mg/Fe-BC led to a slight increase, peaking at 72.2 ± 3.09% on the 17th day and remaining above 60%. Methane content significantly rose with 3% and 5% Mg/

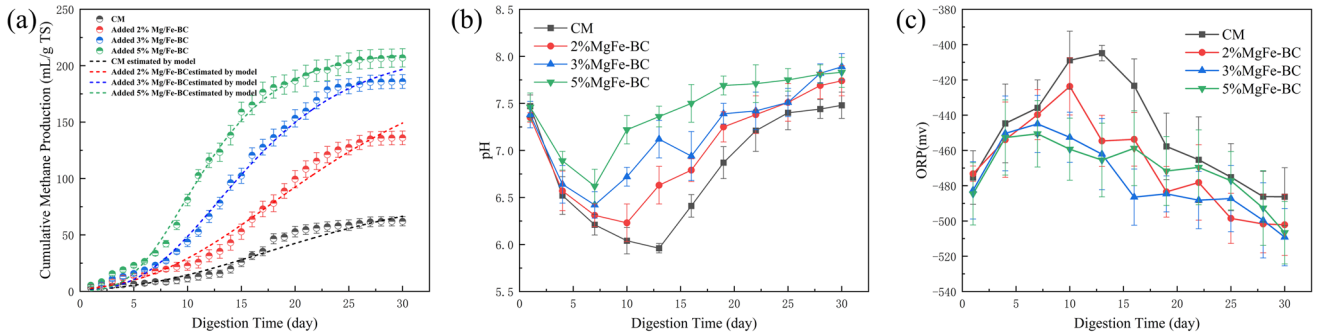

Fig. 5 Methane production kinetics with the addition of Mg/Fe-BC (**a**); pH variations during the anaerobic digestion process (**b**); ORP variations during the anaerobic digestion process (**c**)

Table 5 The kinetics parameters estimated from modified Gompertz model of chicken manure (CM) with increasing Mg/Fe-BC addition

Sample	$P_{(50)}$ (mL/g TS)	P_m (mL/g TS)	R_m (mL/g TS/d)	λ (d)	R^2
CM	62.07±1.08	91.95±10.63	3.04±0.12	13.04±0.57	0.98
Added 2% Mg/Fe-BC	135.98±4.13	171.24±21.47	6.78±0.21	8.78±0.45	0.98
Added 3% Mg/Fe-BC	185.87±4.76	204.75±6.72	11.21±0.39	5.72±0.23	0.99
Added 5% Mg/Fe-BC	206.95±5.52	214.49±2.92	15.86±0.58	4.71±0.22	0.99

Note: $P_{(50)}$ refers to the cumulative methane yield (mL/g TS). P_m refers to the maximum cumulative methane potential (mL/g TS). R_m refers to the maximum methane production rate (mL/g TS/d). λ refers to the lag period (d)

Fe-BC, exceeding 60% on the 9th to 10th day. Throughout anaerobic digestion, average methane proportions with CM-only and 2% Mg/Fe-BC were 35.8% and 54.6% respectively. With 3% and 5% Mg/Fe-BC, the average methane proportions were 58.6% and 61.4%. This demonstrated that Mg/Fe-BC addition not only alleviated severe inhibition but also enhanced methane production [70, 71].

Analysis of Methane Production Kinetics

The Modified Gompertz model was fitted to the cumulative methane production with different additions of Mg/Fe-BC as the anaerobic digestion varied. The results were shown in Fig. 5a, with the corresponding kinetic parameters presented in Table 5. The fitted cumulative methane production displayed an S-shaped trend over time, with correlation coefficients of 0.98, 0.98, 0.99, and 0.99 for CM, 2%, 3%, and 5% Mg/Fe-BC, respectively. This suggested that the model accurately reflected the methane production pattern with the addition of Mg/Fe-BC. The model indicated that the digestion lag time (λ) for CM was 13.04±0.57 days, significantly longer than when 3% and 5% Mg/Fe-BC were added (5.72±0.23d and 4.71±0.22 d, respectively). Although the lag time for 2% Mg/Fe-BC was slightly shorter than CM (λ=8.78±0.45 days), methane production notably increases, aligning with previous biogas production findings. This suggested that CM anaerobic digestion was inhibited by ammonia, resulting in a decrease in the hydrolysis rate. The inclusion of Mg/Fe-BC alleviated inhibition, facilitating a smoother methanogenesis process [72]. After a 30-day period of anaerobic digestion, there was a significant rise in cumulative methane production of around 196-229% with the addition of 3% and 5% Mg/Fe-BC. This indicated a potential influence on NH_4^+-N adsorption, resulting in decreased NH_3 accumulation and improved methane production in the CM anaerobic digestion system [25, 58].

Variations in pH, ORP and VFA

The pH variations during AD with different Mg/Fe-BC additions were illustrated in Fig. 5b. In chicken manure fermentation broth, the pH exhibited a pattern of rapid decline, followed by a gradual recovery, and ultimately stabilized. The pH decline lasted longer for CM-only, with recovery starting after reaching the lowest point (pH=5.96±0.05) on the 13th day of anaerobic digestion. The pH decreased to approximately 6.23±0.05 on the 10th day with 2% Mg/Fe-BC addition, while the pH of the added 3% and 5% Mg/Fe-BC decreased to the lowest value around the 7th day, which coincided with the trend of volatile fatty acid changes later on. Previous research reported that pH levels between 5.8 and 8.5 were suitable for effective anaerobic digestion, with a preference for a neutral pH [73]. Magnesium-iron based biochar employed various mechanisms, such as surface functional groups, metal ion leaching, and ion exchange, to enhance the pH buffering capacity of the anaerobic digestion feedstock system. This helped maintain

pH stability during the anaerobic digestion, preventing dramatic long-term fluctuations [74].

Figure 5c illustrated the variations in ORP values over time during AD for four different groups. In the initial phases of anaerobic digestion, the ORP values of CM and 2% Mg/Fe-BC increased sharply during 1–10 days and then decreased slowly, whereas the ORP of 3% and 5% Mg/Fe-BC reached the maximum value on the 7th day. By the end of the 30d experiment, the ORP values for CM, 2%, 3%, and 5% Mg/Fe-BC were −486.28 ± 16.47 mV, -502.17 ± 17.32 mV, -509.17 ± 16.25 mV, and −506.63 ± 17.73 mV, respectively. Throughout the entire anaerobic digestion process, the ORP value of the Mg/Fe BC addition group remained lower than that of the CM group. The decrease in ORP promoted the conversion of acetic acid and butyric acid, creating a favorable substrate environment for methane production [75].

Figure 6a-d displayed the variations in VFA concentrations during anaerobic digestion. The total VFA concentration peaked during the methanogenesis phase, which was consistent with the trend of cumulative biogas and methane production in Fig. 4a&b. At the peak of VFA accumulation, the total VFA concentrations in fermentation groups with 2%, 3%, and 5%Mg/Fe-BC reached 11446.05 ± 929.31 mg/L, 9589.70 ± 755.54 mg/L, and 8145.18 ± 604.71 mg/L, respectively. It was obvious that the higher the Mg/Fe-BC dosage, the lower the total VFA concentration. As the anaerobic digestion time prolonged, VFA gradually degraded, which was consistent with the previously reported research results [75]. In contrast, the total concentration of VFA in CM was as high as 12825.17 ± 633.78 mg/L, and remained higher than the fermentation group with modified biochar added during the same fermentation period. The VFA components were mainly composed of acetic acid and butyric acid. CM-only accumulated to its maximum value within the first 13 days, and the introduction of Mg/Fe BC led to a decrease in the total accumulation, which corresponded well to the trend of pH changes. Acetic acid and butyric acid gradually decreased over time, indicating their effective conversion into biogas. Previous research reports had shown that propionic acid was an important intermediate in anaerobic digestion, and its accumulation severely hinders methane production [76].

Figure 6a&b showed that the propionate content of CM-only reached its highest level (2855.26 ± 206.85 mg/L) on the 13th day, while the propionate content of 2% Mg/Fe BC reached its peak (2468.69 ± 185.74 mg/L) on the 4th day. After that, the propionate concentration showed a slight downward trend, suggesting that the duration of the lag period was related to the initial propionate concentration. Similarly, from Fig. 6c&d, it could be seen that the highest concentrations of propionate observed in the 3% Mg/Fe-BC and 5% Mg/Fe-BC groups were 2009.61 ± 154.64 mg/L and 1895.38 ± 113.86 mg/L on the 7th day, respectively. It was speculated that methane production was less likely to be inhibited by propionate, as the cumulative methane production in all four groups increases rapidly after the lag period. Although there was a certain correlation with the initial concentration of propionate, long-term AD would reduce the level of propionate, implying that the inhibitory factors in CM anaerobic digestion did not stem from the accumulation of volatile fatty acids, particularly propionate [77].

COD Removal and TAN Variations

The variation of COD concentration and removal efficiency were shown in Fig. 7a. The initial substrate COD concentrations were 32.53 ± 1.25 g/L, 33.68 ± 1.08 g/L, 31.57 ± 1.14 g/L, and 32.88 ± 1.88 g/L for CM, 2%, 3%, and 5% Mg/Fe-BC, respectively. After 4 days of hydrolysis, the COD concentration reached the maximum value (34.69 ± 1.84, 36.25 ± 2.14, 34.43 ± 1.67, and 35.66 ± 1.85 g/L respectively). As the process of AD advanced, organic matter was gradually consumed and degraded, resulting in a dramatic decrease in COD concentration. The 2%, 3%, and 5% Mg/Fe-BC groups had significantly lower COD levels compared to the CM-only. By the 30th day, the COD concentrations were 14.49 ± 1.94 g/L, 11.22 ± 0.5 g/L, 9.28 ± 0.47 g/L, and 9.06 ± 0.46 g/L, respectively, implying that Mg/Fe-BC addition improved acidification, hydrolysis, and methanogenesis efficiency. The COD removal efficiency increased over time, with degradation rates initially slower between 1 and 7 days and then gradually accelerating. The degradation rate of the 2%, 3%, and 5% Mg/Fe-BC groups was higher than that of the CM group. After 30 days of AD, the COD removal efficiency for the 2%, 3%, and 5% Mg/Fe-BC groups reached 66.68 ± 2.64%, 70.59 ± 2.57%, and 72.46 ± 3.14%, respectively, compared to 55.47 ± 3.12% for the CM group. These results indicated that the addition of Mg/Fe-BC enhanced COD removal and substrate degradation efficiency [78].

Due to CM being a substrate with high nitrogen content, the large amount of ammonia nitrogen generated during CM hydrolysis can lead to AD inhibition. Ammonia nitrogen levels exceeding 3.0 g/L have been shown to hinder methane production [79–81]. As shown in Fig. 7b, the initial concentration range of TAN for all four groups was approximately 1.67–1.88 g/L, but it rose rapidly post-hydrolysis. By the 4th day, the TAN concentration in the group treated with 2% Mg/Fe-BC reached around 2.74 ± 0.31 g/L, surpassing the levels observed in the 3% and 5% Mg/Fe-BC groups (approximately 2.43–2.36 g/L). In contrast, the TAN concentration in the CM-only group remained at 3.2 ± 0.13 g/L. The anaerobic digestion of CM-only encountered substantial ammonia inhibition during the initial 13 days, leading

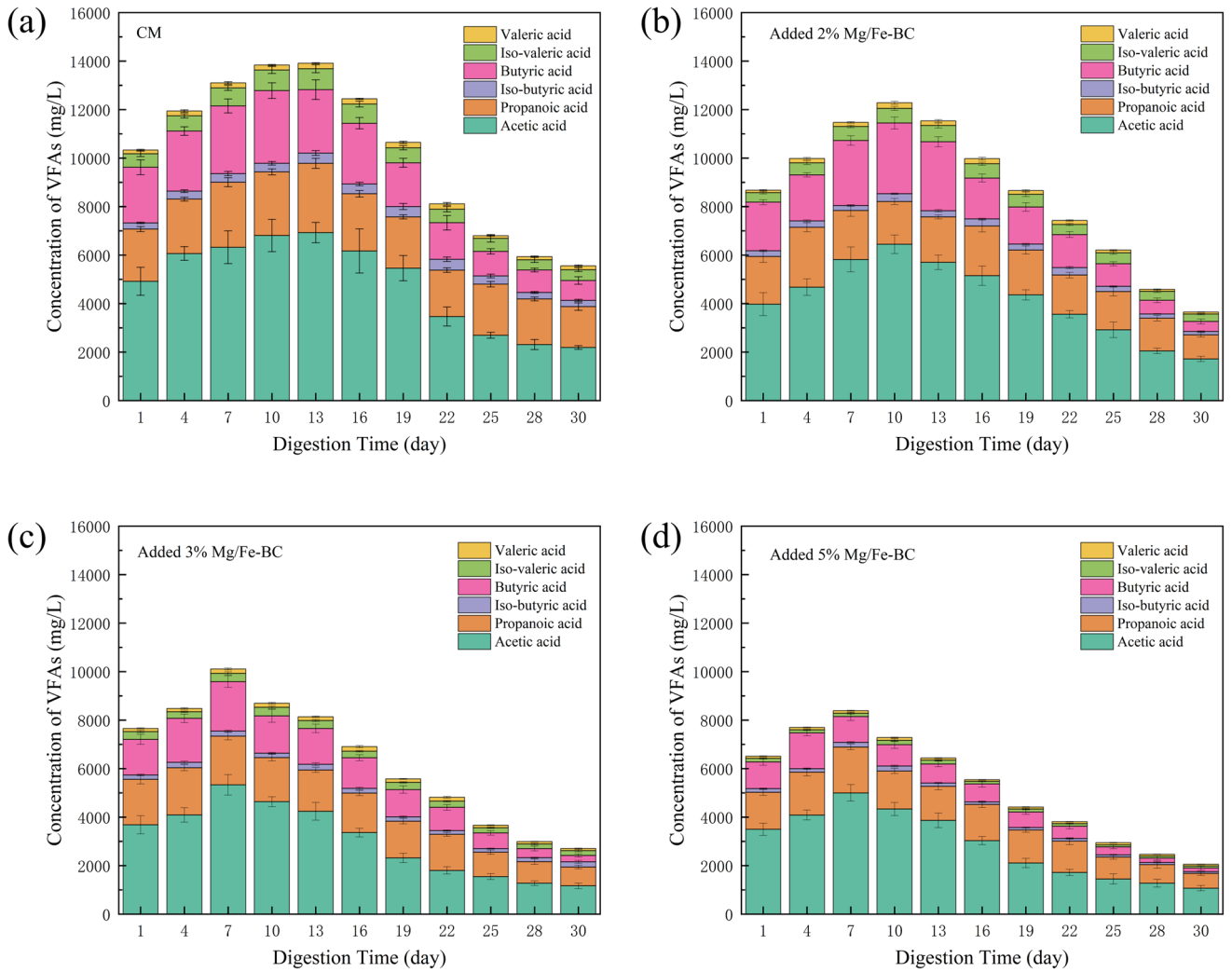

Fig. 6 Variations in VFA during anaerobic digestion with different Mg/Fe-BC additions. (**a**)CM-only; (**b**)added 2%Mg/Fe-BC; (**c**) added 3%Mg/Fe-BC; (**d**) added 5%Mg/Fe-BC

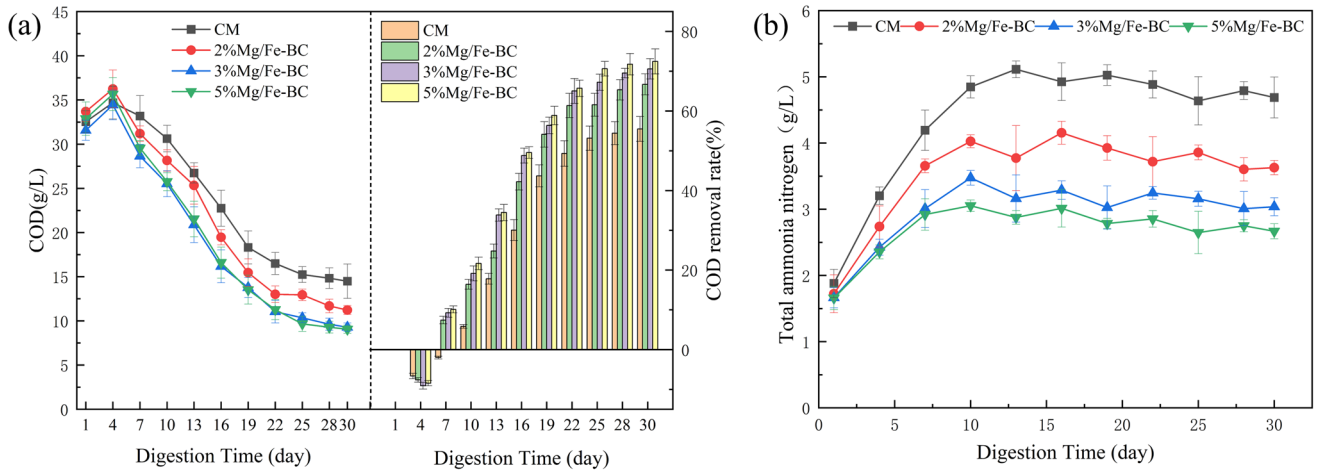

Fig. 7 The impact of Mg/Fe-BC addition on COD concentration and removal rate (**a**); the impact of Mg/Fe-BC addition on total ammonia nitrogen (**b**)

to inconsistent digestion performance. Even on the 30th day, TAN levels remained as high as 4.69 ± 0.31 g/L, indicating sustained inhibition of methane production. The 2% Mg/Fe-BC group was slightly higher than the threshold of ammonia inhibition level (3.63 ± 0.11 g/L), suggesting a possible mild hindrance to methane generation. During AD, the TAN concentrations in the 3% and 5% Mg/Fe-BC groups decreased to 3.04 ± 0.14 g/L and 2.67 ± 0.11 g/L, respectively, approaching the threshold levels. This suggested that the inhibitory effect of ammonia progressively decreased with an increase in the Mg/Fe-BC dosage. Consequently, it had been further substantiated that incorporating 3% and 5% Mg/Fe-BC could alleviate ammonia inhibition during the anaerobic digestion of chicken manure.

Microbial Community Analysis

Bacterial Community

Figure 8a illustrated the community abundance at the bacterial phylum level. The three predominant bacterial phylum were *Bacteroidota,Firmicutes*, and *Synergistota*. Members of *Bacteroidetes* were known to participate in the degradation of complex organic polymers in the digestive system, facilitating the conversion of polysaccharides into acetate and butyrate [82–83]. No significant differences were observed in the relative abundance of *Bacteroidota* across the four groups of anaerobic reactors, with a consistent range of approximately 36-38%. This suggested that the addition of Mg/Fe-BC did not result in a specific enrichment of *Bacteroides*. The relative abundance of *Firmicutes* ranged from 28 to 42%, and these bacteria released extracellular enzymes such as lysozyme, which effectively degraded and hydrolyzed complex organic macromolecules like cellulose, proteins, and lipids. Notably, the abundance of *Synergistota* (9-15%), *Proteobacteria* (2-4%), and *Actinobacteriota* (2-4%) increased significantly following the addition of Mg/Fe-BC. They played crucial roles in the hydrolysis process. *Synergistota* was primarily responsible for promoting the production of VFAs and was also an important electrochemically active bacterial phylum. Some genera of Proteobacteria may be related to methanogens acting as electron donors to enhance the DIET process [84]. In the 3%Mg/Fe-BC and 5%Mg/Fe-BC groups, the relative abundance of *Proteobacteria* was approximately 4%, whereas it was notably lower in the other groups, suggesting an enhanced DIET in the 3%Mg/Fe-BC and 5%Mg/Fe-BC supplementation groups. *Actinobacteriota* had facilitated the degradation of cellulose and carbohydrates, with the relative abundance in the 3% and 5%Mg/Fe-BC addition groups being approximately 3% and 4%, respectively. This facilitative effect indicated that organic waste was more readily decomposed into VFAs [85]. Furthermore, the abundance of *Cloacimonadota* was about 2% after the addition of Mg/Fe-BC, which was not detected in the CM group because it had a certain alleviating effect on the toxicity of ammonia nitrogen [86].

At the genus level, *Ignatzschineria,Romboutsia,Fastidiosipila*, and *Bacteroides* were the predominant bacterial genera in AD system, collectively accounting for a relative abundance of approximately 39-45% (Fig. 8b). *Romboutsia* was capable of degrading complex organic matter, while *Fastidiosipila* could hydrolyze and utilize proteins containing alanine, phenylalanine, and proline. *Bacteroides* facilitated the production of short-chain fatty acids, such as succinate, acetate, and butyrate, which were the primary end products [87, 88]. Notably, *Syntrophomonas* and *Geobater* were present in the Mg/Fe-BC group but were almost undetectable in the CM only group. They were typical electron donor bacteria involved in DIET and were able to establish DIET with *Methanosaeta* to increase methane production [70]. This suggested that the addition of Mg/Fe-BC enhanced the capacity of DIET in the AD system, thereby increasing the conversion of VFAs to methane. In addition, there was a slight increase in the abundance of *Clostridium_sensu_stricto_1* after the addition of Mg/Fe-BC, which might be associated with the production of acetic acid and propionic acid, suggesting that their elevated abundance might increase methane production during AD.

Archaeal Community

As shown in Fig. 8c&d, a total of 4 archaea phylum and 8 archaea genus were detected in the collected biogas slurry. At the phylum level, *Euryarchaeota,Crenarchaeota,Nanoarchaeaeota*, and *Thaumarchaeota* were the predominant archaea in AD. After the addition of Mg/Fe-BC, the relative abundance of the predominant archaeal phylum *Euryarchaeota* and *Crenarchaeota* increased marginally by 2–3% in comparison to the CM group. This phenomenon may be attributed to the enhanced methane production facilitated by methanogenic archaea [83]. At the genus level, *Methanosarcina,Methanoculleus,Methanosaeta,Methanobacterium*, and *Bathyarchaeia* were the predominant archaea. *Methanosarcina* was a mixed-nutrient methanogenic bacterium capable of generating methane using carbon dioxide or acetate and possesses the ability of DIET [82]. Additionally, previous studies had reported that *Methanosarcina* could also utilize butyric acid to promote methane generation [89]. In this study, the abundance of *Methanosarcina* in both the CM and Mg/Fe-BC reactors remained consistently high, further substantiating its capability to efficiently utilize acetic acid and butyric acid, as well as its resilience to high concentrations of AN, VFAs, and other inhibitory

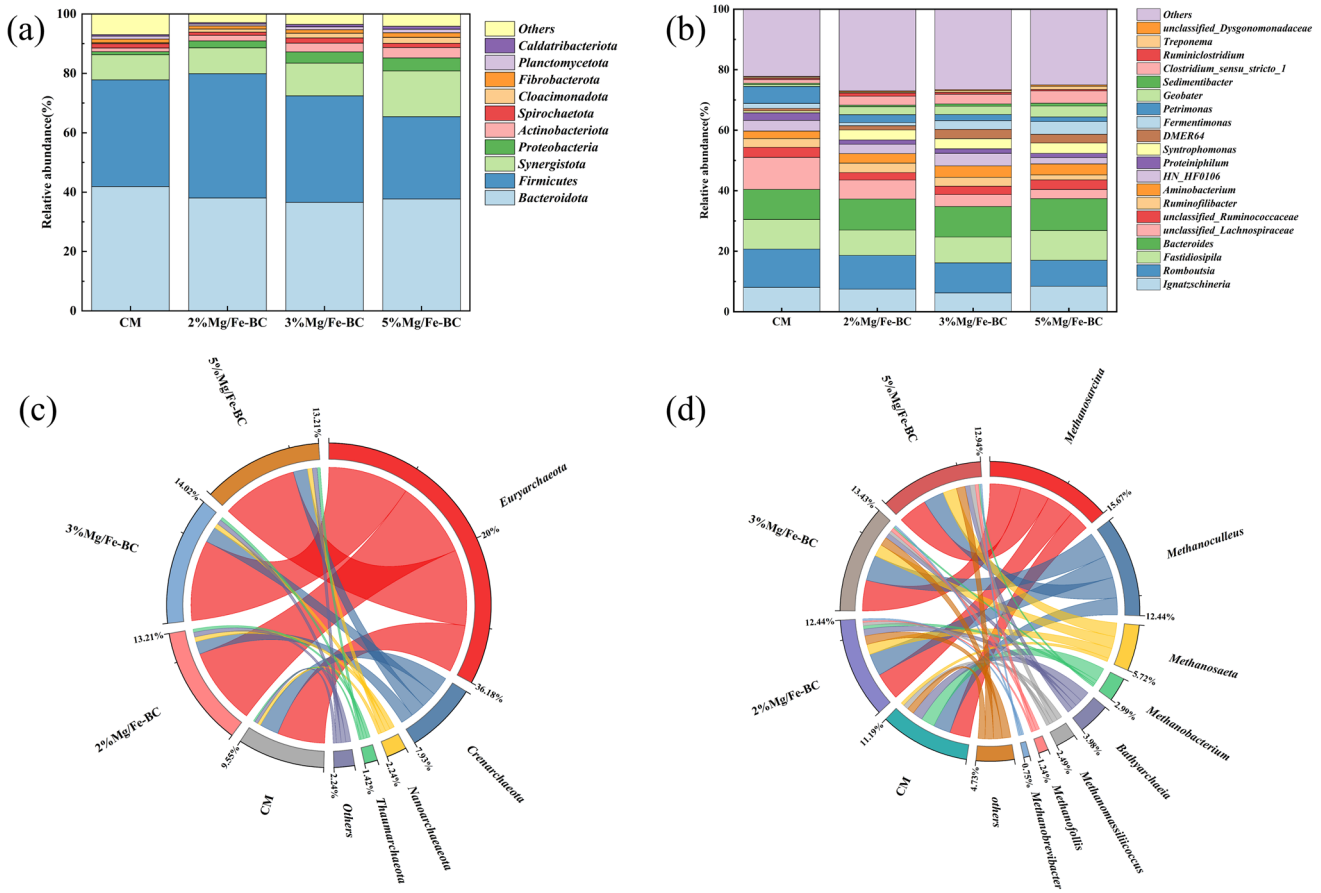

Fig. 8 Relative abundance of (**a**) bacterial communities at the phylum level, (**b**) bacterial communities at the genus level, (**c**) archaeal community at the phylum level and (**d**) archaeal community at the genus level

substances. *Methanoculleus*, a hydrogenotrophic methanogen, was capable of synthesizing methane from hydrogen or formate and carbon dioxide. The introduction of Mg/Fe-BC led to a slight increase in the abundance of *Methanoculleus*, suggesting a correlation between methane production and the enrichment of hydrogenotrophic *Methanoculleus* [73]. After the addition of Mg/Fe-BC, there was a significant rise in the abundance of *Methanosaeta*, primarily attributed to its strong affinity for acids, its ability to oxidize electrons, and its competitive edge in low VFA environments [90]. *Bathyarchaeia* possessed multiple methanogenic pathways, such as hydrogenotrophic, methylotrophic, and acetotrophic methanogenesis, enabling it to produce methane even under conditions of elevated ammonia nitrogen levels. This was corroborated by the observed reduction in the abundance of *Bathyarchaeia* after Mg/Fe-BC addition [84]. *Methanobacterium*, a hydrogenotrophic methanogenic bacterium, primarily generated methane via H_2 or formic acid. Consequently, it was present exclusively in the CM reactor, while its presence appeared to be minimal in the Mg/Fe-BC reactor, aligning with previous research findings [76].

Conclusions

In this study, magnesium-iron modified biochar was successfully prepared through co-precipitation and post-pyrolysis. Mg/Fe-BC exhibited a higher specific surface area and crystallinity compared to Mg-BC and Fe-BC, and was found to be rich in various acidic functional groups. In a simulated solution containing ammonia nitrogen with an initial concentration of 120 mg/L and a dosage of 1 g/L, the maximum adsorption capacity of Mg/Fe BC evaluated by isothermal adsorption was 87.83 mg/g. The pseudo-second-order kinetic model predicted that the process was mainly chemical adsorption dominated by ion exchange. In actual chicken manure digestate, the removal efficiency of ammonia nitrogen exceeded 30% with the addition of 3% Mg/Fe-BC. AD results indicated that cumulative methane production increased by 116-229% as Mg/Fe-BC dosage increased from 2 to 5%. Mg/Fe-BC effectively mitigated ammonia nitrogen inhibition in the AD of chicken manure, leading to significant reductions in anaerobic parameters such as VFA, COD content, and ORP. Ammonia nitrogen concentration remained below threshold levels, ensuring a

stable and controllable anaerobic reaction system. The analysis of microbial community structure revealed that Mg/Fe-BC could alter the composition of the archaeal community and enhance the relative abundance of methanogenic bacteria and archaea. This study provided valuable insights into the technological process of AD of chicken manure, thereby facilitating the utilization of poultry farm waste and contributing to the management of environmental pollution. Future research will investigate the metabolic intermediates and microbial community structure in the AD of chicken manure to further elucidate the enhancement mechanism of magnesium-iron modified biochar.

Supplementary Information The online version contains supplementary material available at https://doi.org/10.1007/s12649-025-02894-0.

Acknowledgements The authors would like to express their gratitude for the financial support provided by Gansu Major Science and Technology Projects (22ZD6WA056) and Gansu Province Higher Education Industry Support and Guidance Project (2022CYZC-28) and Modern Silk Road Cold and Drought Agricultural Science and Technology Support Project (GSLK-2022-19) and Science and Technology Plan Project of Gannan (2023JY1SC002) and Gansu Provincial Youth Science and Technology Fund Program Project (21JR7RF886) and Jiuquan Science and Technology Support Program (2023CA2014 and 2024CA1083).

Author Contributions All authors contributed to the study conception and design. Material preparation, data collection and analysis were performed by Tao Li and Tingting Li. Supervision and validation were by Jinping Li and Xiuwen Cheng. The first draft of the manuscript was written by Tao Li and all authors commented on previous versions of the manuscript. All authors read and approved the final manuscript.

Funding The authors have no relevant financial or non-financial interests to disclose.

Data Availability Data will be made available on request.

Declarations

Ethical Approval This declaration is not applicable since no human and animal studies were carried out.

Competing Interests The authors declare no competing interests.

References

1. Xu, R., Zhang, Y.R., Xiong, W.P., Sun, W.M., Fan, Q., Yang, Z.H.: Metagenomic approach reveals the fate of antibiotic resistance genes in a temperature-raising anaerobic digester treating municipal sewage sludge. J. Clean. Prod. **277**, 123504 (2020). https://doi.org/10.1016/j.jclepro.2020.123504
2. Deng, Y.F., Xia, J., Zhao, R., Xu, J.X., Liu, X.Y.: Iron-coated biochar alleviates acid accumulation and improves methane production under ammonium enrichment conditions. Sci. Total Environ. **809**, 151154 (2022). https://doi.org/10.1016/j.scitotenv.2021.151154
3. Cheng, H.H., Narindri, B., Chu, H., Whang, L.M.: Recent advancement on biological technologies and strategies for resource recovery from swine wastewater. Bioresour Technol. **303**, 122861 (2020). https://doi.org/10.1016/j.biortech.2020.122861
4. Usman Khan, M., Kiaer Ahring, B.: Improving the biogas yield of manure: Effect of pretreatment on anaerobic digestion of the recalcitrant fraction of manure. Bioresour Technol. **321**, 124427 (2021). https://doi.org/10.1016/j.biortech.2020.124427
5. Hoyos-Sebá, J.J., Arias, N.P., Salcedo-Mendoza, J., Aristizábal-Marulanda, V.: Animal manure in the context of renewable energy and value-added products: A review. Chem. Eng. Prog. **196**, 109660 (2024). https://doi.org/10.1016/j.cep.2023.109660
6. Wu, S.H., Shen, Z.Q., Yang, C.P., Zhou, Y.X., Li, X., Zeng, G.M., Ai, S.J., He, H.J.: Effects of C/N ratio and bulking agent on speciation of Zn and Cu and enzymatic activity during pig manure composting. Int. Biodeterior. Biodegrad. **119**, 429–436 (2017). https://doi.org/10.1016/j.ibiod.2016.09.016
7. Zhou, Q., Li, X., Wu, S.H., Zhong, Y.Y., Yang, C.P.: Enhanced strategies for antibiotic removal from swine wastewater in anaerobic digestion. Trends Biotechnol. **39**(1), 8–11 (2021). https://doi.org/10.1016/j.tibtech.2020.07.002
8. Hill, A., Tait, S., Baillie, C., Virdis, B., McCabe, B.: Microbial electrochemical sensors for volatile fatty acid measurement in high strength wastewaters: A review. Biosens. Bioelectron. **165**, 112409 (2020). https://doi.org/10.1016/j.bios.2020.112409
9. Huang, Z.W., Niu, Q.Y., Nie, W.K., Li, X., Yang, C.P.: Effects of heavy metals and antibiotics on performances and mechanisms of anaerobic digestion. Bioresour Technol. **361**, 127683 (2022). https://doi.org/10.1016/j.biortech.2022.127683
10. Li, Q., Xu, M.J., Wang, G.J., Chen, R., Qiao, W., Wang, X.C.: Biochar assisted thermophilic co-digestion of food waste and waste activated sludge under high feedstock to seed sludge ratio in batch experiment. Bioresour Technol. **249**, 1009–1016 (2018). https://doi.org/10.1016/j.biortech.2017.11.002
11. Tao, B., Donnelly, J., Oliveira, I., Anthony, R., Wilson, V., Esteves, S.R.: Enhancement of microbial density and methane production in advanced anaerobic digestion of secondary sewage sludge by continuous removal of ammonia. Bioresour Technol. **232**, 380–388 (2017). https://doi.org/10.1016/j.biortech.2017.02.066
12. Wang, W., Ren, X.S., Yang, K., Hu, Z.H., Yuan, S.J.: Inhibition of ammonia on anaerobic digestion of synthetic coal gasification wastewater and recovery using struvite precipitation. J. Hazard. Mater. **340**, 152–159 (2017). https://doi.org/10.1016/j.jhazmat.2017.07.002
13. Rodriguez-Verde, I., Regueiro, L., Lema, J.M., Carballa, M.: Blending based optimisation and pretreatment strategies to enhance anaerobic digestion of poultry manure. Waste Manage. **71**, 521–531 (2018). https://doi.org/10.1016/j.wasman.2017.11.002
14. Kumar, M., Dutta, S., You, S.M., Luo, G., Zhang, S.C., Show, P.L., Sawarkar, A.D., Singh, L., Tsang, D.C.W.: A critical review on biochar for enhancing biogas production from anaerobic digestion of food waste and sludge. J. Clean. Prod. **305**, 127143 (2021). https://doi.org/10.1016/j.jclepro.2021.127143
15. Zhang, M., Song, G., Gelardi, D.L., Huang, L.B., Khan, E., Mašek, O., Parikh, S.J., Ok, Y.S.: Evaluating biochar and its modifications for the removal of ammonium, nitrate, and phosphate in water. Water Res. **186**, 116303 (2020). https://doi.org/10.1016/j.watres.2020.116303
16. Liu, Y.W., Li, X., Wu, S.H., Tan, Z., Yang, C.P.: Enhancing anaerobic digestion process with addition of conductive materials. Chemosphere. **278**, 130449 (2021). https://doi.org/10.1016/j.chemosphere.2021.130449
17. Romero-Güiza, M.S., Vila, J., Mata-Alvarez, J., Chimenos, J.M., Astals, S.: The role of additives on anaerobic digestion: A review. Renew. Sust Energ. Rev. **58**, 1486–1499 (2016). https://doi.org/10.1016/j.rser.2015.12.094

18. Farghali, M., Chen, Z., Osman, A.I., Ali, I.M., Hassan, D., Ihara, I., Rooney, D.W., Yap, P.S.: Strategies for ammonia recovery from wastewater: A review. Environ. Chem. Lett. **22**, 2699–2751 (2024). https://doi.org/10.1007/s10311-024-01768-6
19. He, Q.S., Li, X.F., Ren, Y.P.: Analysis of the simultaneous adsorption mechanism of ammonium and phosphate on magnesium-modified biochar and the slow release effect of fertilizer. Biochar. **4**(1), 25 (2022). https://doi.org/10.1007/s42773-022-00150-5
20. Akor, C.I., Osman, A.I., Farrell, C., McCallum, C.S., Doran, W.J., Morgan, K., Harrison, J., Walsh, P.J., Sheldrake, G.N.: Thermokinetic study of residual solid digestate from anaerobic digestion. Chem. Eng. J. **406**, 127039 (2021). https://doi.org/10.1016/j.cej.2020.127039
21. Osman, A.I., Elgarahy, A.M., Mehta, N., Al-Muhtaseb, A.H., Al-Fatesh, A.S., Rooney, D.W.: Facile synthesis and life cycle assessment of highly active magnetic sorbent composite derived from mixed plastic and biomass waste for water remediation. ACS Sustainable Chem. Eng. **10**(37), 12433–12447 (2022). https://doi.org/10.1021/acssuschemeng.2c04095
22. Jiao, Y.X., Li, D.Y., Wang, M., Gong, T.C., Sun, M.Y., Yang, T.X.: A scientometric review of biochar preparation research from 2006 to 2019. Biochar. **3**(3), 283–298 (2021). https://doi.org/10.1007/s42773-021-00091-5
23. Khoshnevisan, B., Duan, N., Tsapekos, P., Awasthi, M.K., Liu, Z., Mohammadi, A., Angelidaki, I., Tsang, D.C.W., Zhang, Z., Pan, J.T., Ma, L., Aghbashlo, M., Tabatabaei, M., Liu, H.B.: A critical review on livestock manure biorefinery technologies: Sustainability, challenges, and future perspectives. Renew. Sust Energ. Rev. **135**, 110033 (2021). https://doi.org/10.1016/j.rser.2020.110033
24. Yu, Q., Sun, C., Liu, R.H., Yellezuome, D., Zhu, X.P., Bai, R.F., Liu, M.Q., Sun, M.Z.: Anaerobic co-digestion of corn stover and chicken manure using continuous stirred tank reactor: The effect of biochar addition and urea pretreatment. Bioresour Technol. **319**, 124197 (2021). https://doi.org/10.1016/j.biortech.2020.124197
25. Pan, J.T., Ma, J.Y., Liu, X.X., Zhai, L.M., Ouyang, X.H., Liu, H.B.: Effects of different types of biochar on the anaerobic digestion of chicken manure. Bioresour Technol. **275**, 258–265 (2019). https://doi.org/10.1016/j.biortech.2018.12.068
26. Zhu, X., Labianca, C., He, M., Luo, Z., Wu, C., You, S., Tsang, D.C.W.: Life-cycle assessment of pyrolysis processes for sustainable production of biochar from agro-residues. Bioresour Technol. **360**, 127601 (2022). https://doi.org/10.1016/j.biortech.2022.127601
27. Feng, Q., Chen, M., Wu, P., Zhang, X., Wang, S., Yu, Z., Wang, B.: Simultaneous reclaiming phosphate and ammonium from aqueous solutions by calcium alginate-biochar composite: Sorption performance and governing mechanisms. Chem. Eng. J. **429**, 132166 (2022). https://doi.org/10.1016/j.cej.2021.132166
28. Rahman, S., Navarathna, C.M., Krishna Das, N., Alchouron, J., Reneau, P., Stokes, S., Thirumalai, R.V.K.G., Perez, F., Barbary Hassan, E., Mohan, D., Pittman, C.U., Mlsna, T.: High capacity aqueous phosphate reclamation using Fe/Mg-layered double hydroxide (LDH) dispersed on biochar. J. Colloid Interface Sci. **597**, 182–195 (2021). https://doi.org/10.1016/j.jcis.2021.03.114
29. Bian, H., Shen, C., Liu, W., Man, Y.B., Wong, M.H., Christie, P., Shan, S., Wang, M., Zhang, J.: An improved method of MgFe-layered double hydroxide/ biochar composite synthesis. J. Clean. Prod. **393**, 136186 (2023). https://doi.org/10.1016/j.jclepro.2023.136186
30. He, L.T., Wang, D.H., Wu, Z.Y., Lv, Y.Z., Li, S.C.: Magnesium-modified biochar was used to adsorb phosphorus from wastewater and used as a phosphorus source to be recycled to reduce the ammonia nitrogen of piggery digestive wastewater. J. Clean. Prod. **360**, 132130 (2022). https://doi.org/10.1016/j.jclepro.2022.132130
31. Gahlot, P., Ahmed, B., Tiwari, S.B., Aryal, N., Khursheed, A., Kazmi, A.A., Tyagi, V.K.: Conductive material engineered direct interspecies electron transfer (DIET) in anaerobic digestion: Mechanism and application. Environ. Technol. Innov. **20**, 101056 (2020). https://doi.org/10.1016/j.eti.2020.101056
32. Samuel Olugbenga, O., Goodness Adeleye, P., Blessing Oladipupo, S., Timothy Adeleye, A., Igenepo John, K.: Biomass-derived biochar in wastewater treatment a circular economy approach. Waste Manage. Bull. **1**(4), 1–14 (2024). https://doi.org/10.1016/j.wmb.2023.07.007
33. Hu, Y., Zhu, Y., Zhang, Y., Lin, T., Zeng, G., Zhang, S., Wang, Y., He, W., Zhang, M., Long, H.: An efficient adsorbent: Simultaneous activated and magnetic ZnO doped biochar derived from camphor leaves for ciprofloxacin adsorption. Bioresour Technol. **288**, 121511 (2019). https://doi.org/10.1016/j.biortech.2019.121511
34. Ji, X., Liu, Y., Gao, Z., Lin, H., Xu, X., Zhang, Y., Zhu, K., Zhang, Y., Sun, H., Duan, J.: Efficiency and mechanism of adsorption for imidacloprid removal from water by Fe-Mg co-modified water hyacinth-based biochar: Batch adsorption, fixed-bed adsorption, and DFT calculation. Sep. Purif. Technol. **330**, 125235 (2024). https://doi.org/10.1016/j.seppur.2023.125235
35. Fawzy, S., Osman, A.I., Mehta, N., Moran, D., Al-Muhtaseb, A.H., Rooney, D.W.: Atmospheric carbon removal via industrial biochar systems: A techno-economic-environmental study. J. Cean Prod. **371**, 133660 (2022). https://doi.org/10.1016/j.jclepro.2022.133660
36. Li, D., Chen, L., Liu, X.F., Mei, Z.L., Ren, H.W., Cao, Q., Yan, Z.Y.: Instability mechanisms and early warning indicators for mesophilic anaerobic digestion of vegetable waste. Bioresour Technol. **245**, 90–97 (2017). https://doi.org/10.1016/j.biortech.2017.07.098
37. Pasalari, H., Esrafili, A., Rezaee, A., Gholami, M., Farzadkia, M.: Electrochemical oxidation pretreatment for enhanced methane potential from landfill leachate in anaerobic co-digestion process: Performance, Gompertz model, and energy assessment. Chem. Eng. J. **422**, 130046 (2021). https://doi.org/10.1016/j.cej.2021.130046
38. Liu, Y.K., Ying, L.X., Li, H., Awasthi, M.K., Tian, D., Zou, J.M., Lei, Y.J., Shen, F.: Allophane improves anaerobic digestion of chicken manure by alleviating ammonia inhibition and intensifying direct interspecies electron transfer. Bioresour Technol. **400**, 130692 (2024). https://doi.org/10.1016/j.biortech.2024.130692
39. Wakudkar, H., Jain, S.: A holistic overview on corn cob biochar: A mini-review. Waste Manage. Res. **40**(8), 1143–1155 (2022). https://doi.org/10.1177/0734242X211069741
40. Spokas, K.A.: Review of the stability of biochar in soils: Predictability of O:C molar ratios. Carbon Manage. **1**(2), 289–303 (2010). https://doi.org/10.4155/CMT.10.32
41. Rong, X., Xie, M., Kong, L.S., Natarajan, V., Ma, L., Zhan, J.H.: The magnetic biochar derived from banana peels as a persulfate activator for organic contaminants degradation. Chem. Eng. J. **372**, 294–303 (2019). https://doi.org/10.1016/j.cej.2019.04.135
42. Cai, Y., Zhu, M., Meng, X., Zhou, J.L., Zhang, H., Shen, X.: The role of biochar on alleviating ammonia toxicity in anaerobic digestion of nitrogen-rich wastes: A review. Bioresour Technol. **351**, 126924 (2022). https://doi.org/10.1016/j.biortech.2022.126924
43. Gu, X.H., Li, H., Shi, Y.X., Li, J.J., Li, S.Y.: Regulating bacterial dynamics by Mg-modified biochar addition to mitigate gaseous emissions during pig manure composting. J. Clean. Prod. **465**, 142839 (2024). https://doi.org/10.1016/j.jclepro.2024.142839
44. Wang, C., Liu, Y., Wang, C., Xing, B., Zhu, S., Huang, J., Xu, X., Zhu, L.: Biochar facilitates rapid restoration of methanogenesis by enhancing direct interspecies electron transfer after high organic loading shock. Bioresour Technol. **320**, 124360 (2021). https://doi.org/10.1016/j.biortech.2020.124360

45. He, L.T., Wang, D.H., Wu, Z.Y., Li, S.C., Lv, Y.Z.: Co-pyrolysis of pig manure and magnesium-containing waste residue and phosphorus recovery for planting feed corn. J. Water Process. Eng. **49**, 103146 (2022). https://doi.org/10.1016/j.jwpe.2022.103146
46. Huang, X., Wei, D., Zhang, X.W., Fan, D.W., Sun, X., Du, B., Wei, Q.: Synthesis of amino-functionalized magnetic aerobic granular sludge-biochar for pb(II) removal: Adsorption performance and mechanism studies. Sci. Total Environ. **685**, 681–689 (2019). https://doi.org/10.1016/j.scitotenv.2019.05.429
47. Liang, M.N., Xu, S.P., Zhu, Y.N., Chen, X., Deng, Z.L., Yan, L.L., He, H.J.: Preparation and characterization of Fe-Mn binary oxide/mulberry stem biochar composite adsorbent and adsorption of cr(VI) from aqueous solution. Int. J. Environ. Res. Public. Health. **17**(3), 676 (2020). https://doi.org/10.3390/ijerph17030676
48. Shakoor, M.B., Ye, Z.L., Chen, S.H.: Engineered biochars for recovering phosphate and ammonium from wastewater: A review. Sci. Total Environ. **779**, 146240 (2021). https://doi.org/10.1016/j.scitotenv.2021.146240
49. Tang, Y., Zhang, S.H., Su, Y.L., Wu, D., Zhao, Y.P., Xie, B.: Removal of microplastics from aqueous solutions by magnetic carbon nanotubes. Chem. Eng. J. **406**, 126804 (2021). https://doi.org/10.1016/j.cej.2020.126804
50. Mohan, D., Pittman, C.U., Bricka, M., Smith, F., Yancey, B., Mohammad, J., Steele, P.H., Alexandre-Franco, M.F., Gómez-Serrano, V., Gong, H.: Sorption of arsenic, cadmium, and lead by chars produced from fast pyrolysis of wood and bark during bio-oil production. J. Colloid Interf Sci. **310**(1), 57–73 (2007). https://doi.org/10.1016/j.jcis.2007.01.020
51. Masebinu, S.O., Akinlabi, E.T., Muzenda, E., Aboyade, A.O.: A review of biochar properties and their roles in mitigating challenges with anaerobic digestion. Renew. Sust Energ. Rev. **103**, 291–307 (2019). https://doi.org/10.1016/j.rser.2018.12.048
52. Osman, A.I., Lai, Z.Y., Farghali, M., Yiin, C.L., Elgarahy, A.M., Hammad, A., Ihara, I., Al-Fatesh, A.S., Rooney, D.W., Yap, P.S.: Optimizing biomass pathways to bioenergy and biochar application in electricity generation, biodiesel production, and biohydrogen production. Environ. Chem. Lett. **21**(5), 2639–2705 (2023). https://doi.org/10.1007/s10311-023-01613-2
53. Zhang, T., Wu, X., Shaheen, S.M., Zhao, Q., Liu, X., Rinklebe, J., Ren, H.: Ammonium nitrogen recovery from digestate by hydrothermal pretreatment followed by activated hydrochar sorption. Chem. Eng. J. **379**, 122254 (2020). https://doi.org/10.1016/j.cej.2019.122254
54. Li, B.T., Jing, F.Y., Hu, Z.Q., Liu, Y.X., Xiao, B., Guo, D.B.: Simultaneous recovery of nitrogen and phosphorus from biogas slurry by Fe-modified biochar. J. Saudi Chem. Soc. **25**(4), 101213 (2021). https://doi.org/10.1016/j.jscs.2021.101213
55. Zhang, N., Zheng, H.Y., Hu, X.H., Zhu, Q., Stanislaus, M.S., Li, S.Y., Zhao, C.Y., Wang, Q.H., Yang, Y.N.: Enhanced bio-methane production from ammonium-rich waste using eggshell-and lignite-modified zeolite (ELMZ) as a bio-adsorbent during anaerobic digestion. Process. Biochem. **81**, 148–155 (2019). https://doi.org/10.1016/j.procbio.2019.03.001
56. Li, H.B., Wang, Y.W., Zhao, Y.W., Wang, L., Feng, J.T., Sun, F.: Efficient simultaneous phosphate and ammonia adsorption using magnesium-modified biochar beads and their recovery performance. J. Environ. Chem. Eng. **11**(5), 110875 (2023). https://doi.org/10.1016/j.jece.2023.110875
57. Bian, H.H., Wang, M.Y., Han, J.L., Hu, X.P., Xia, H.L., Wang, L., Fang, C.C., Shen, C., Man, Y.B., Wang, M.H., Shan, S.D., Zhang, J.: MgFe-LDH@biochars for removing ammonia nitrogen and phosphorus from biogas slurry: Synthesis routes, composite performance, and adsorption mechanisms. Chemosphere. **324**, 138333 (2023). https://doi.org/10.1016/j.chemosphere.2023.138333
58. Ngo, T., Shahsavari, E., Shah, K., Surapaneni, A., Ball, A.S.: Improving bioenergy production in anaerobic digestion systems utilising chicken manure via pyrolysed biochar additives: A review. Fuel. **316**, 123374 (2022). https://doi.org/10.1016/j.fuel.2022.123374
59. Wang, B., Lehmann, J., Hanley, K., Hestrin, R., Enders, A.: Adsorption and desorption of ammonium by maple wood biochar as a function of oxidation and pH. Chemosphere. **138**, 120–126 (2015). https://doi.org/10.1016/j.chemosphere.2015.05.062
60. Li, A., Ge, W., Liu, L., Qiu, G.: Preparation, adsorption performance and mechanism of MgO-loaded biochar in wastewater treatment: A review. Environ. Res. **212**, 113341 (2022). https://doi.org/10.1016/j.envres.2022.113341
61. Mia, S., Dijkstra, F.A., Singh, B.: Aging Induced changes in Biochar's functionality and adsorption behavior for phosphate and ammonium. Environ. Sci. Technol. **51**(15), 8359–8367 (2017). https://doi.org/10.1021/acs.est.7b00647
62. Thi Mai, V., Van Tuyen, T., Dinh Phuong, D., Huu Tap, V., Tien Vinh, N., Vigneswaran, S., Huu Hao, N.: Removing ammonium from water using modified corncob-biochar. Sci. Total Environ. **579**, 612–619 (2017). https://doi.org/10.1016/j.scitotenv.2016.11.050
63. Ngo, D.N.G., Chuang, X.Y., Huang, C.P., Hua, L.C., Huang, C.: Compositional characterization of nine agricultural waste biochars: The relations between alkaline metals and cation exchange capacity with ammonium adsorption capability. J. Environ. Chem. Eng. **11**(3), 110003 (2023). https://doi.org/10.1016/j.jece.2023.110003
64. Fotidis, I.A., Karakashev, D., Kotsopoulos, T.A., Martzopoulos, G.G., Angelidaki, I.: Effect of ammonium and acetate on methanogenic pathway and methanogenic community composition. Fems Microbiol. Ecol. **83**(1), 38–48 (2013). https://doi.org/10.1111/j.1574-6941.2012.01456.x
65. Paritosh, K., Yadav, M., Chawade, A., Sahoo, D., Kesharwani, N., Pareek, N., Vivekanand, V.: Additives as a support structure for specific biochemical activity boosts in anaerobic digestion: A review. Front. Energy Res. **8**, 88 (2020). https://doi.org/10.3389/fenrg.2020.00088
66. Fagbohungbe, M.O., Herbert, B.M.J., Hurst, L., Ibeto, C.N., Li, H., Usmani, S.Q., Semple, K.T.: The challenges of anaerobic digestion and the role of biochar in optimizing anaerobic digestion. Waste Manage. **61**, 236–249 (2017). https://doi.org/10.1016/j.wasman.2016.11.028
67. Gomez, X., Meredith, W., Fernandez, C., Sanchez-Garcia, M., Diez-Antolinez, R., Garzon-Santos, J., Snape, C.E.: Evaluating the effect of biochar addition on the anaerobic digestion of swine manure: Application of Py-GC/MS. Environ. Sci. Pollut R. **25**(25), 25600–25611 (2018). https://doi.org/10.1007/s11356-018-2644-4
68. Wang, Z.Z., Jiang, Y., Wang, S., Zhang, Y.Z., Hu, Y.S., Hu, Z.H., Wu, G.X., Zhan, X.M.: Impact of total solids content on anaerobic co-digestion of pig manure and food waste: Insights into shifting of the methanogenic pathway. Waste Manage. **114**, 96–106 (2020). https://doi.org/10.1016/j.wasman.2020.06.048
69. Liu, X., Meng, Q.T., Wu, F.J., Zhang, C., Tan, X.J., Wan, C.L.: Enhanced biogas production in anaerobic digestion of sludge medicated by biochar prepared from excess sludge: Role of persistent free radicals and electron mediators. Bioresour Technol. **347**, 126422 (2022). https://doi.org/10.1016/j.biortech.2021.126422
70. Sun, W.X., Fu, S.F., Zhu, R., Wang, Z.Y., Zou, H., Zheng, Y.: Improved anaerobic digestion efficiency of high-solid sewage sludge by enhanced direct interspecies electron transfer with activated carbon mediator. Bioresour Technol. **313**, 123648 (2020). https://doi.org/10.1016/j.biortech.2020.123648
71. Di, L., Zhang, Z.Y., Han, D., Bu, F.F., Wang, H., Deng, X.T.: Review on electricity market reform at home and abroad.

Procedia Comput. Sci. **203**, 375–380 (2022). https://doi.org/10.1016/j.procs.2022.07.048
72. Li, W.L., Lu, C.B., An, G.J., Zhang, Y.M., Tong, Y.W.: Integration of high-solid digestion and gasification to dispose horticultural waste and chicken manure. Chin. J. Chem. Eng. **26**(5), 1145–1151 (2018). https://doi.org/10.1016/j.cjche.2017.09.020
73. Di, L., Wang, F., Li, S.Y., Wang, H., Zhang, D.L., Yi, W.M., Shen, X.L.: Influence of nano-Fe3O4 biochar on the methanation pathway during anaerobic digestion of chicken manure. Bioresour Technol. **377**, 128979 (2023). https://doi.org/10.1016/j.biortech.2023.128979
74. Nie, W.K., He, S.Y., Lin, Y., Cheng, J.J., Yang, C.P.: Functional biochar in enhanced anaerobic digestion: Synthesis, performances, and mechanisms. Sci. Total Environ. **906**, 167681 (2024). https://doi.org/10.1016/j.scitotenv.2023.167681
75. Cheng, J.H., Ye, R.K., Zhu, J., Tang, Y., Huang, S.Q., Ge, D.D., Geng, Z.T.: Effect of ferrite doped sludge-based catalysts on methane production in anaerobic digestion of organic solid waste. Fuel. **368**, 131309 (2024). https://doi.org/10.1016/j.fuel.2024.131309
76. Di, L., Zhang, Q., Wang, F., Wang, H., Liu, H., Yi, W., Zhang, Z., Zhang, D.: Effect of nano-Fe3O4 biochar on anaerobic digestion of chicken manure under high ammonia nitrogen concentration. J. Clean. Prod. **375**, 134107 (2022). https://doi.org/10.1016/j.jclepro.2022.134107
77. Han, Y., Green, H., Tao, W.D.: Reversibility of propionic acid inhibition to anaerobic digestion: Inhibition kinetics and microbial mechanism. Chemosphere. **255**, 126840 (2020). https://doi.org/10.1016/j.chemosphere.2020.126840
78. Yuan, T.G., Bian, S.W., Ko, J.H., Liu, J.G., Shi, X.Y., Xu, Q.Y.: Exploring the roles of zero-valent iron in two-stage food waste anaerobic digestion. Waste Manage. **107**, 91–100 (2020). https://doi.org/10.1016/j.wasman.2020.04.004
79. Ngo, T., Khudur, L.S., Hassan, S., Jansriphibul, K., Ball, A.S.: Enhancing microbial viability with biochar for increased methane production during the anaerobic digestion of chicken manure. Fuel. **368**, 131603 (2024). https://doi.org/10.1016/j.fuel.2024.131603
80. Li, Z.Y., Inoue, D., Ike, M.: Mitigating ammonia-inhibition in anaerobic digestion by bioaugmentation: A review. J. Water Process. Eng. **52**, 103506 (2023). https://doi.org/10.1016/j.jwpe.2023.103506
81. Nie, H., Jacobi, H.F., Strach, K., Xu, C.M., Zhou, H.J., Liebetrau, J.: Mono-fermentation of chicken manure: Ammonia inhibition and recirculation of the digestate. Bioresour Technol. **178**, 238–246 (2015). https://doi.org/10.1016/j.biortech.2014.09.029
82. Niu, Q., Takemura, Y., Kubota, K., Li, Y.Y.: Comparing mesophilic and thermophilic anaerobic digestion of chicken manure: Microbial community dynamics and process resilience. Waste Manage. **43**, 114–122 (2015). https://doi.org/10.1016/j.wasman.2015.05.012
83. Ziganshina, E.E., Ibragimov, E.M., Vankov, P.Y., Miluykov, V.A., Ziganshin, A.M.: Comparison of anaerobic digestion strategies of nitrogen-rich substrates: Performance of anaerobic reactors and microbial community diversity. Waste Manage. **59**, 160–171 (2017). https://doi.org/10.1016/j.wasman.2016.10.038
84. Sitthi, S., Hatamoto, M., Watari, T., Yamaguchi, T.: Accelerating anaerobic propionate degradation and studying microbial community using modified polyvinyl alcohol beads during anaerobic digestion. Bioresour Technol. Rep. **17**, 100907 (2022). https://doi.org/10.1016/j.biteb.2021.100907
85. Qin, S., Wainaina, S., Liu, H., Soufiani, A.M., Pandey, A., Zhang, Z., Awasthi, M.K., Taherzadeh, M.J.: Microbial dynamics during anaerobic digestion of sewage sludge combined with food waste at high organic loading rates in immersed membrane bioreactors. Fuel. **303**, 121276 (2021). https://doi.org/10.1016/j.fuel.2021.121276
86. Liu, Y., Ying, L., Li, H., Awasthi, M.K., Tian, D., He, J., Zou, J., Lei, Y., Shen, F.: Allophane improves anaerobic digestion of chicken manure by alleviating ammonia inhibition and intensifying direct interspecies electron transfer. Bioresour Technol. **400**, 130692 (2024). https://doi.org/10.1016/j.biortech.2024.130692
87. Shin, J.H., Tillotson, G., MacKenzie, T.N., Warren, C.A., Wexler, H.M., Goldstein, E.J.C.: Bacteroides and related species: The keystone taxa of the human gut microbiota. Anaerobe. **85**, 102819 (2024). https://doi.org/10.1016/j.anaerobe.2024.102819
88. Liu, J., Wang, R., Qiu, S., Peng, Y., Peng, Y.: Feasibility of double nitrite supply through partial nitrification and partial denitrification driven by sludge fermentation. Bioresour Technol. **414**, 131580 (2024). https://doi.org/10.1016/j.biortech.2024.131580
89. Rastogi, G., Ranade, D.R., Yeole, T.Y., Patole, M.S., Shouche, Y.S.: Investigation of methanogen population structure in biogas reactor by molecular characterization of methyl-coenzyme M reductase A (mcrA) genes. Bioresour Technol. **99**(13), 5317–5326 (2008). https://doi.org/10.1016/j.biortech.2007.11.024
90. Xu, S., Han, R., Zhang, Y., He, C., Liu, H.: Differentiated stimulating effects of activated carbon on methanogenic degradation of acetate, propionate and butyrate. Waste Manage. **76**, 394–403 (2018). https://doi.org/10.1016/j.wasman.2018.03.037